Mechanism of the lifespan extension induced by submaximal SERCA inhibition in *C. elegans*

Paloma García-Casas, Pilar Alvarez-Illera, Rosalba I Fonteriz, Mayte Montero and Javier Alvarez*

Institute of Biology and Molecular Genetics (IBGM), Department of Biochemistry and Molecular Biology and Physiology, Faculty of Medicine, University of Valladolid and CSIC, Ramón y Cajal, 7, E-47005 Valladolid, SPAIN.

***Corresponding autor. E-mail address:** jalvarez@ibgm.uva.es

Keywords: *C. elegans*; SERCA; thapsigargin; lifespan; endoplasmic reticulum; mitochondria; AMP kinase; TOR

Abbreviations: ER, endoplasmic reticulum; SERCA, Sarco Endoplasmic Reticulum Ca^{2+} ATPase; AMPK, AMP-activated protein kinase; TOR, target of rapamycin; TORC1, TOR complex 1; $InsP_3R$, inositol 1,4,5-trisphosphate receptors; RyR, ryanodine receptors; MAMs, mitochondria-associated ER membranes; STIM, stromal interaction molecule; NGM, nematode growth medium; 2,5-BHQ, 2,5-di-tert-butylhydroquinone; GFP, green fluorescent protein.

Highlights

- Submaximal SERCA inhibition with inhibitors or RNAi increases C. elegans lifespan.
- Lifespan extension required functional mitochondria, and both AMPK and TOR pathways.
- Instead, the insulin signaling pathway and the sirtuin pathway were not involved.
- ER-mitochondria Ca^{2+} signaling may play a role in the aging process.
- The SERCA pump may be a new pharmacological target to act on longevity.

Abstract

We have reported recently that submaximal inhibition of the Sarco Endoplasmic Reticulum Ca^{2+} ATPase (SERCA) produces an increase in the lifespan of *C. elegans* worms. We have explored here the mechanism of this increased survival by studying the effect of SERCA inhibition in several mutants of signaling pathways related to longevity. Our data show that the mechanism of the effect is unrelated with the insulin signaling pathway or the sirtuin activity, because SERCA inhibitors increased lifespan similarly in mutants of these pathways. However, the effect required functional mitochondria and both the AMP kinase and TOR pathways, as the SERCA inhibitors were ineffective in the corresponding mutants. The same effects were obtained after reducing SERCA expression with submaximal RNAi treatment. The SERCA inhibitors did not induce ER-stress at the concentrations used, and their effect was not modified by inactivation of the OP50 bacterial food. Altogether, our data suggest that the effect may be due to a reduced ER-mitochondria Ca^{2+} transfer acting via AMPK activation and mTOR inhibition to promote survival.

1. INTRODUCTION

The molecular mechanisms that modulate aging and longevity are starting to be uncovered mainly thanks to studies in model organisms such as the nematode *C. elegans*. These studies have revealed that several metabolic signaling pathways play a crucial role to control lifespan. These signaling pathways include the insulin/insulin-like growth factor, the AMP-activated protein kinase (AMPK), the target of rapamycin (TOR), the sirtuins and mitochondrial respiration and function (López-Otín et al., 2013; Riera et al., 2016). *C. elegans* strains with mutations in different components of these pathways have become essential to investigate the involvement of these pathways in the regulation of longevity and the interrelationships among them. For example, mutations in the insulin-like receptor (*daf-2*) nearly double lifespan, while mutations in its downstream transcription factor DAF-16/FOXO (negatively regulated by the insulin-like receptor) significantly reduce lifespan (Castillo-Quan et al., 2015; Lapierre and Hansen, 2012; Mukhopadhyay et al., 2006). Similarly, mutations in the AMPK α-subunits reduce *C. elegans* lifespan, while mutations in the TOR pathway increase it (Blackwell et al., 2019; Castillo-Quan et al., 2015; Lapierre and Hansen, 2012). Knock-out of the sirtuin gene SIR-2.1 shortens lifespan (Castillo-Quan et al., 2015; Mukhopadhyay et al., 2006), and many mutations in the mitochondrial respiratory chain lead to an increased lifespan (Wang and Hekimi, 2015).

These pathways do not work isolated, instead they keep complex interactions at several levels that sometimes make difficult to evaluate the role of a particular pathway in a given phenomenon. Among others, Ca^{2+} signaling appears to be one of the key factors controlling the function and interconnection of these signaling pathways related to longevity. In particular, AMPK, TOR and mitochondrial function appear to be the main routes controlled by Ca^{2+}, although the precise mechanisms are still not well understood.

The canonical mechanism for activation of AMPK includes phosphorylation by Ca^{2+}-calmodulin protein kinase β, so that an increase in cytosolic Ca^{2+} should activate AMPK (Jeon, 2016; Woods et al., 2005). In addition, AMPK is a well-characterized cellular energy sensor, which becomes activated by increases in the AMP/ATP ratio (Jeon, 2016). As the rate of mitochondrial ATP production is controlled by the mitochondrial [Ca^{2+}], changes in the mitochondrial Ca^{2+} fluxes also modulate AMPK activation. In turn, it has been recently described that AMPK activates the mitochondrial Ca^{2+} uniporter, thus facilitating Ca^{2+} entry into mitochondria to increase ATP production (Zhao et al., 2019). On the other hand, AMPK reduces endoplasmic reticulum (ER) Ca^{2+} release by inhibiting either inositol 1,4,5-trisphosphate receptors ($InsP_3R$) (Arias-del-Val et al., 2019) or ryanodine receptors (RyR) (Yavari et al., 2017), but upregulates SERCA2a in mice hearts (Morissette et al., 2019). This kind of effects may modulate the ER to mitochondria Ca^{2+} transfer, a Ca^{2+} flux that seems to have very important roles in the control of mitochondrial metabolism and autophagy (Ahumada-Castro et al., 2019; Gomez-Suaga et al., 2017). Finally, AMPK has been recently associated to store operated Ca^{2+} entry via modulation of STIM, the ER Ca^{2+}-sensor responsible of activating Ca^{2+} entry through the plasma membrane after ER Ca^{2+} depletion.

AMPK-mediated phosphorylation of STIM1 has been reported to inhibit the store-operated Ca^{2+} entry (Nelson et al., 2019), while Ca^{2+}-mediated activation of AMPK is regulated by binding of AMPK to STIM2 (Chauhan et al., 2019).

The effects of Ca^{2+} on TOR signaling are less clear. AMPK inhibits the TORC1 complex, and therefore Ca^{2+}-induced AMPK activation should inhibit TORC1 (Bootman et al., 2018), although the mechanism of this effect is unclear in *C. elegans* (Blackwell et al., 2019). However, some studies have also shown a direct activation of TOR by cytosolic Ca^{2+} increases, induced either by amino acids (Carroll et al., 2015) or by physical exercise (Ito et al., 2013). In addition, TOR has also been shown to activate plasma membrane store-operated Ca^{2+} channels (Ogawa et al., 2012; Peng et al., 2013) and $InsP_3$ receptors in the ER (MacMillan et al., 2005; Régimbald-Dumas et al., 2011), favoring the increase in cytosolic $[Ca^{2+}]$.

Therefore, changes in cytosolic and mitochondrial $[Ca^{2+}]$ regulate in a complex manner the activity of these two essential kinases, AMPK and TOR, and Ca^{2+} dynamics in these compartments depends directly on ER $[Ca^{2+}]$ levels, ER Ca^{2+} release and ER to mitochondria Ca^{2+} transfer. We have recently described that submaximal concentrations of inhibitors of the SERCA pump increase the lifespan in *C. elegans* worms (García-Casas et al., 2018). In this work, we have investigated further the mechanism of this effect by studying the effects of the SERCA inhibitors in several *C. elegans* mutants of different signaling pathways related to longevity. We have also obtained similar effects on lifespan using submaximal SERCA (*sca-1*) RNAi, confirming that the effect of SERCA inhibitors is due to SERCA inhibition. We suggest that the increase in lifespan induced by SERCA inhibitors may be mediated by a decrease in the ER to mitochondria Ca^{2+} transfer, leading to AMPK activation and TOR block.

2. MATERIALS AND METHODS

2.1 *C. elegans* strains and maintenance.

The effect of the SERCA inhibition on *C. elegans* lifespan was studied in the following mutant strains: *nuo-6(qm200)*, *daf-15(m81)/unc-24(e138)*, *daf-2(e1370), daf-16(mu86), aak-1(tm1944);aak-2(ok524)*, and *sir-2.1(ok434)*, *mcu-1(ju1154)* and *unc-68(r1161).* The strain SJ4005 (*zcIs4 [hsp-4::GFP*]), kindly supplied by Dr. Malene Hansen, Sanford Burnham Prebys Medical Discovery Institute, La Jolla, USA, was used to measure ER stress. The other strains were obtained from the Caenorhabditis Genetics Center. Worms were maintained and handled on NGM agar plates seeded with Escherichia coli (OP50), as previously described (Stiernagle, 2006).

2.2 Administration of the SERCA inhibitors and RNAi.

2,5-di-tert-butylhydroquinone (2,5-BHQ) was dissolved directly in the Nematode Growth Medium (NGM) agar by strong stirring at 250μM. In the case of thapsigargin, it was added

directly to the plate. 10µl of 10µM thapsigargin were added on top of the 10ml OP50-seeded NGM agar to obtain a final concentration (assuming homogeneous distribution) of 10nM.

The HT115 RNAi clone for *sca-1* (K11D9.2, Ahringer library) and empty vector (L4440) were kindly provided by Dr. Malene Hansen. HT115 *sca-1* RNAi and L4440 bacteria were cultured overnight at 37ºC in LB medium containing 125µM ampicillin. Once they reached a DO_{595} = 0.6, *sca-1* RNAi and empty vector L4440 bacteria were mixed to the desired percentage and then 100µl of the mixture were seeded onto 35mm plates containing NGM agar with 1mM isopropyl-b-D-thiogalactoside (IPTG), 50µM carbenicillin and 30µM fluorodeoxyuridine, and incubated for 3 days at 20ºC. Ten young adult worms (day 1) were then transferred onto the plates for lifespan assays.

2.3 *C. elegans* lifespan assay

Synchronized eggs were obtained as described previously (Stiernagle, 2006) and transferred to NGM plates seeded with *E. coli* (OP50), either control plates or plates prepared in the presence of the required drug. 15µM Fluorodeoxyuridine was added to every plate to avoid progeny. For each lifespan assay, at least 10 synchronized young adults (day 1) were transferred to each *E. coli* (OP50) seeded NGM plate (35 mm plates, 10 plates per condition with 10 worms/plate, at least 100 worms per condition). Control and drug-containing assays were always carried out in parallel and kept together in the incubator set at 20ºC. Plates were scored for dead worms every day. Worms that did not respond to touch with a platinum wire were considered dead. Age refers to days following adulthood. Missing worms, individuals with extruded gonad or desiccated by crawling in the edge of the plate were censored, as well as plates with fungal contamination during the first 10 days. Statistics was made with the SPSS software using the Kaplan-Meier estimator and the log-rank routine for significance.

For the experiments with dead bacteria, OP50 were grown overnight at 37ºC and then heat inactivated at 65ºC for 30 min. The resulting heat-killed bacteria were used to seed NGM plates and the rest of the assay was as described above. These experiments were carried out using the AQ2038 (N2 expressing the YC2.1 Ca^{2+} sensor in the pharynx, (Alvarez-Illera et al., 2016) strain as a control. Its lifespan was not significantly different from that of the N2 strain (data not shown).

2.4 *C. elegans* ER stress measurement by fluorescence.

ER stress was measured in the strain SJ4005 (*zcIs4 [hsp-4::GFP*]) (Kapulkin et al., 2005), which contains a GFP reporter transgene under the control of the *hsp-4* promoter. Induction of ER stress leads to a strong increase in GFP expression, reflecting the upregulation of the hsp-4 gene. Worms were treated as described above with the SERCA inhibitors or with the corresponding amount of DMSO for the controls. After 3 days, some worms of each plate were transferred to plates with 10µg/ml tunicamycin and the same treatments, to obtain the maximum possible induction. Fluorescence images were then taken 6h afterword using a Leica M165 FC stereo microscope equipped with a Leica DFC7000 T camera. Analysis of the images was made by calculating the mean fluorescence of 40-42 worms of each condition using ImageJ. Significance was obtained with the ANOVA test.

2.5. RT-qPCR.

RT-qPCR was performed as described previously (Alvarez-Illera et al., 2020). Worms at day 5 of adult life were harvested by centrifugation and washed with water. Total RNA was obtained by freeze/thaw using Trizol (Invitrogen, Waltham, MA, USA) and homogenization using the Minibeadbeater-8, and RNA was then extracted using the RNeasy mini kit (Qiagen, Madrid, Spain), treated with the RNase-Free DNase Set (Qiagen) and then precipitated with ethanol and resuspended in water. RNA concentrations and quality were measured using a NanoDrop spectrophotometer. Reverse transcription reaction was carried out with the iScript™ cDNA Synthesis Kit (BioRad, Madrid, Spain) using random primers. RT-qPCR was carried out using the LightCycler 480 PCR system (Roche Applied Science). Reactions were performed using the SYBR Green Master Mix (Applied Biosystems/Thermo Fisher Scientific, Waltham, MA, USA) using the following primers: *hsp-3*; forward, ACCGTCACCATCCAGGTC; reverse, TCCGGTGAGGTCGAACTTT (Kozlowski et al., 2014). *hsp-4*; forward, ACGACCACAATCGTCTCAGTCC; reverse, CTTCGTCAGTGAGCTTTCCTCC (Kozlowski et al., 2014). *sca-1*; forward, CTTCCAGCCACTGCTCTCGGATTC; reverse, CTGGTAGTAGGTGATCTGTGGTCC. The actin 1 gene (*act-1*) was used as the endogenous control gene. The following program parameters were used for all amplifications: 95°C for 10 min, followed by 45 cycles at 95°C for 15s, 60°C for 30s and 72ºC for 30s, and finally one cycle at 95°C for 20 min, 65°C for 1 min, and 97°C for 5 min. Assays were performed using three biological replicates, each consisting of technical triplicates.

2.6 Materials.

2,5-BHQ (code 419648) was from Sigma-Aldrich, Madrid, Spain. Thapsigargin was from Abcam, Madrid, Spain. FuDR was from Alfa Aesar, Karlsruhe, Germany. Other reagents were from Sigma, Madrid, Spain or Merck, Darmstadt, Germany.

3. RESULTS

We have reported before that the SERCA inhibitors thapsigargin and 2,5-BHQ produce an 10-15% increase in lifespan in wild-type *C. elegans* worms. Similar effects were obtained in the *eat-2(ad1113)* strain (García-Casas et al., 2018), which has a defect in pharynx pumping that leads to dietary restriction and lifespan increase (Jia and Levine, 2007). This suggested that the mechanism of the effect of the SERCA inhibitors was not related with dietary restriction, but gave no further clues on what could be the real mechanism. We have then studied here the effect of the SERCA inhibitors in several mutants of signaling pathways known to be related to longevity.

3.1 Effect of SERCA inhibitors on *C. elegans* mutants of the insulin or sirtuin signaling pathways.

We first studied their effect in two mutants on the insulin signaling pathway. The DAF-2 gene encodes for the insulin-like growth factor 1 (IGF-1) receptor and the *daf-2(e1370)* mutant shows a severe disruption of this pathway that leads to an important extension of the lifespan (Dorman et al., 1995). Activation of the IGF-1 receptor triggers a signaling cascade including activation of phosphoinositide 3-kinase and Akt/Protein Kinase B, that ends up by

phosphorylating the transcription factor DAF-16/FOXO, that in this form remains inactive in the cytosol (Sun et al., 2017). In the absence of IGF-1 signaling (e.g., in *daf-2* mutants), DAF-16 dephosphorylates, enters the nucleus and activates a transcriptional program that nearly doubles worms lifespan (Kenyon et al., 1993). Fig. 1, panels a-b, shows that the SERCA inhibitors extended the lifespan of *daf-2* mutants as much as in the wild-type (García-Casas et al., 2018), in spite of the much larger lifespan of these mutants. Thapsigargin increased lifespan by 13.0±2.5% and 2,5-BHQ by 11.4±1.3%, in both cases with all the trials statistically significant (see Table S1a). Therefore, our data suggest that the increase in lifespan induced by the SERCA inhibitors is independent or additive to that induced when the DAF-16 transcription factor enters the nucleus. However, SERCA inhibitors produced a much smaller effect in *daf-16* mutants (Fig. 1, panels c-d). These mutants have a shorter lifespan, and thapsigargin only increased it by 7.1±2.0%, with only 2 of the 3 trials significant. Similarly, 2,5-BHQ increased lifespan by only 5.1±4.7%, with 2 of the 3 trials significant (see Table S1b). Therefore, the absence of the DAF-16 transcription factor partially impairs the effect of the SERCA inhibitors. This means that at least part of the effect of the SERCA inhibitors requires the presence of DAF-16/FOXO.

We have then explored the involvement of sirtuins by using the *sir-2.1* mutant. The SIR-2.1 gene is a homologous of human SIRT1, it has histone deacetylase activity and is involved in longevity. In particular, it is required for lifespan extension by caloric restriction, independent of the insulin/IGF-1 signaling pathway, and the *sir-2.1* mutant has a slight decrease in lifespan (Wang and Tissenbaum, 2006). Fig. 1, panels e-f and table S1c show the effects of the SERCA inhibitors in this mutant. Thapsigargin extended the lifespan by 9.4±0.9%, with all the 3 trials significant and 2,5-BHQ extended lifespan by 10.2±5.9%, although only 2 of the trials produced significant differences. The effects are therefore similar to those obtained in the wild-type (García-Casas et al., 2018), suggesting that SIR-2.1 is not involved in the effect of the SERCA inhibitors.

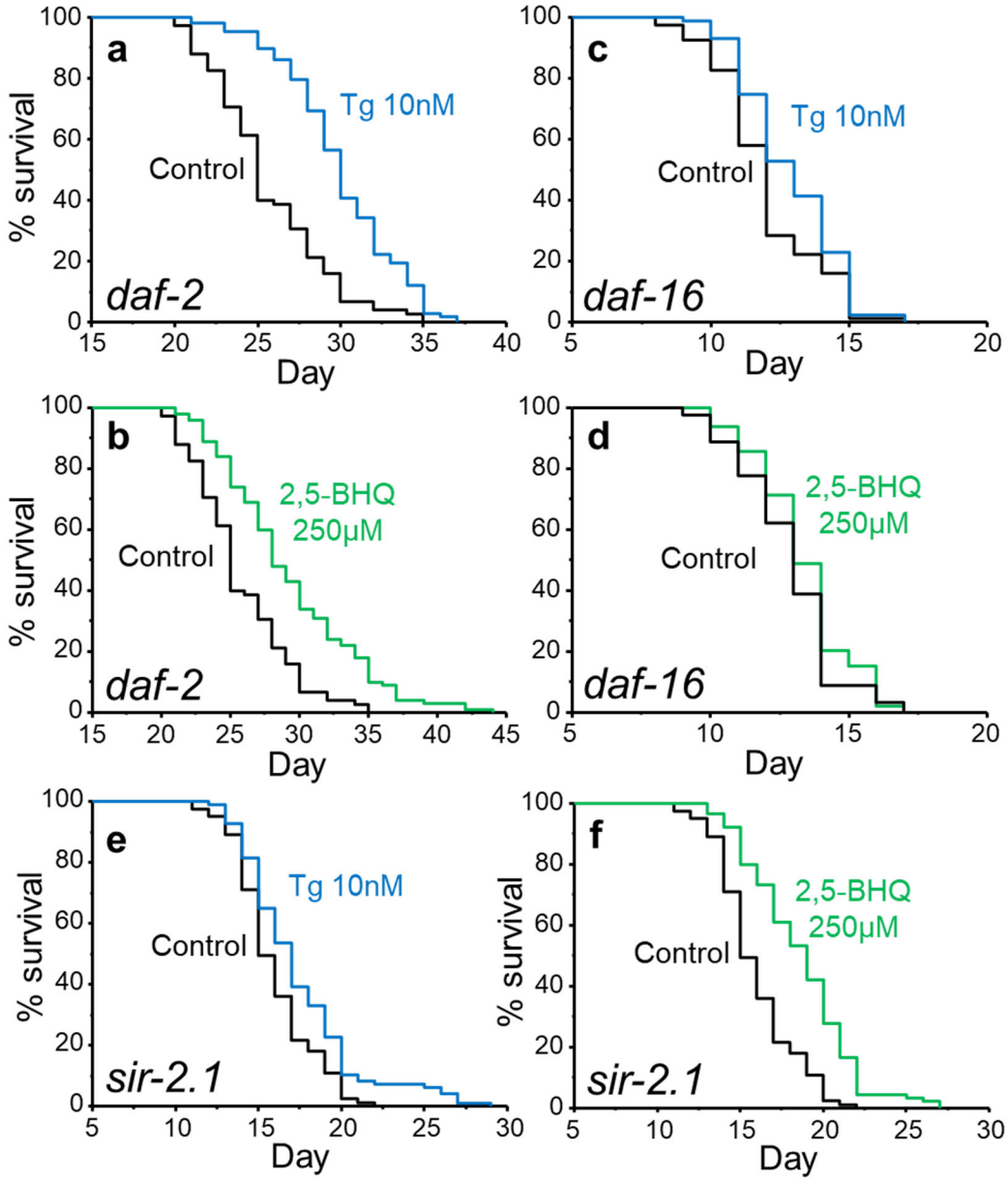

Figure 1. Effect of SERCA inhibitors on the lifespan of *daf-2*, *daf-16* and *sir-2.*1 mutants. Panels show representative survival plots corresponding to parallel lifespan trials (control vs drug) performed in *daf-2* mutants (panels a-b), *daf-16* mutants (panels c-d) and sir-2.1 mutants (panels e-f) using either 10nM thapsigargin (panels a,c,e) or 250µM 2,5-BHQ (panels b,d,f). In each panel, the trace labelled "Control" was obtained with the corresponding mutant, and the other was obtained in the same mutant treated with the indicated drug from day 1 of adult life. The trials shown correspond to those marked in bold in Table S1 (more details and statistics of all the assays in Table S1).

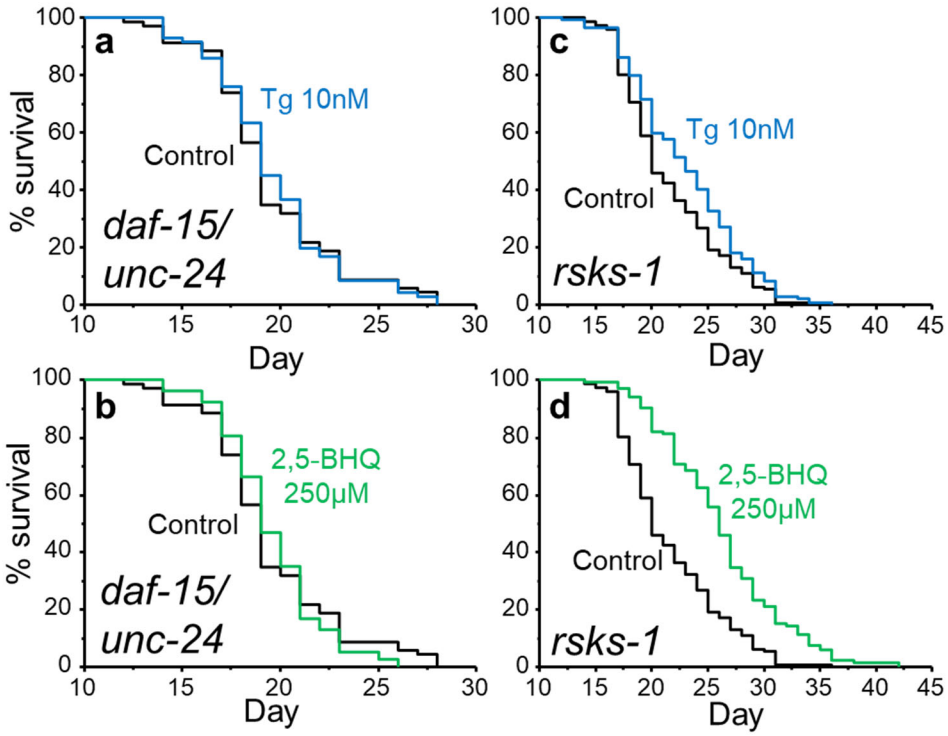

Figure 2. Effect of SERCA inhibitors on the lifespan of *daf-15/unc-24* and *rsks-1* mutants. Panels show representative survival plots corresponding to parallel lifespan trials (control vs drug) performed in *daf-15/unc-24* mutants (panels a-b) and *rsks-1* mutants (panels c-d) using either 10nM thapsigargin (panels a,c) or 250µM 2,5-BHQ (panels b,d). In each panel, the trace labelled "Control" was obtained with the corresponding mutant, and the other was obtained in the same mutant treated with the indicated drug from day 1 of adult life. The trials shown correspond to those marked in bold in Table S2 (more details and statistics of all the assays in Tables S1 and S2).

3.2 Effect of SERCA inhibitors on *C. elegans* mutants of the TOR pathway.

The possible involvement of the TOR pathway has been investigated using two different mutants, *daf-15/unc-24* and *rsks-1*. The DAF-15 gene encodes for the RAPTOR-like subunit of TORC1 in *C. elegans*. Homozygotic *daf-15* mutants are dauer constitutive, but heterocygotes show a significant reduction in the activity of the pathway and increase in lifespan, and combination with *unc-24* facilitates strain maintenance (Jia et al., 2004). Fig. 2, panels a-b, shows that none of the SERCA inhibitors produced any effect in the heterocygote *daf-15/unc-24* mutant (see table S2a for more details). Therefore, the TORC1 activity is necessary for the effect of the SERCA inhibitors. Regarding the RSKS-1 gene, it is a homologous of the S6 kinase (S6K), one of the main downstream targets of TORC1. In this mutant, the SERCA inhibitors were instead very effective. Thapsigargin produced an increase in lifespan similar to that observed in the wild-type (García-Casas et al., 2018), 10.1±2.1%, with all the trials significant, and 2,5-BHQ induced a much larger increase in lifespan of almost 25% (see fig 2, panels c-d, and table S2b).

S6K has been reported to be essential to mediate lifespan extension by dietary restriction via HIF-1 and PHA-4-dependent mechanisms (Kapahi et al., 2010). In this sense, the fact that thapsigargin and 2,5-BHQ are still effective in the *rsks-1* mutant is consistent with the fact that they were also effective in the *eat-2* dietary restriction mimicking mutant (García-Casas et al., 2018). In conclusion, the effects of the SERCA inhibitors requires the presence of TORC1, but it is not mediated by S6K. As an alternative, the effect could be mediated by the inhibitory interaction between TORC1 and DAF-16 (Zhao and Wang, 2016).

3.3 Effect of SERCA inhibition with RNAi on *C. elegans* lifespan.

To obtain further evidence for the involvement of the SERCA Ca^{2+} pump in the effect of thapsigargin and 2,5-BHQ, we used RNAi against the only SERCA gen present in C. elegans, known as SCA-1. Loss of function mutation of *sca-1* results in embryonic and larval lethality (Cho et al., 2000; Zwaal et al., 2001). Therefore, we decided to assay several dilutions of *sca-1* RNAi to search for the one able to mimic the effect of the SERCA inhibitors. Fig. 3 shows that 5 and 10% dilutions of *sca-1* RNAi increased *C. elegans* lifespan by about 20%, while dilutions above 25% reduced *C. elegans* lifespan by a similar amount (see Table S3 form more details). Therefore, partial reduction of *sca-1* expression also increased *C. elegans* lifespan, confirming that the effect of submaximal concentrations of thapsigargin and 2,5-BHQ is mediated by inhibition of SERCA. Fig. 3d shows the effects of 10% and 100% *sca-1* RNAi on the SCA-1 mRNA expression. In the presence of 10% *sca-1* RNAi, SCA-1 mRNA expression was reduced to 27±2% of the control, and 100% *sca-1* RNAi reduced SCA-1 mRNA expression to 13±4% of the control (mean±s.e., n=3).

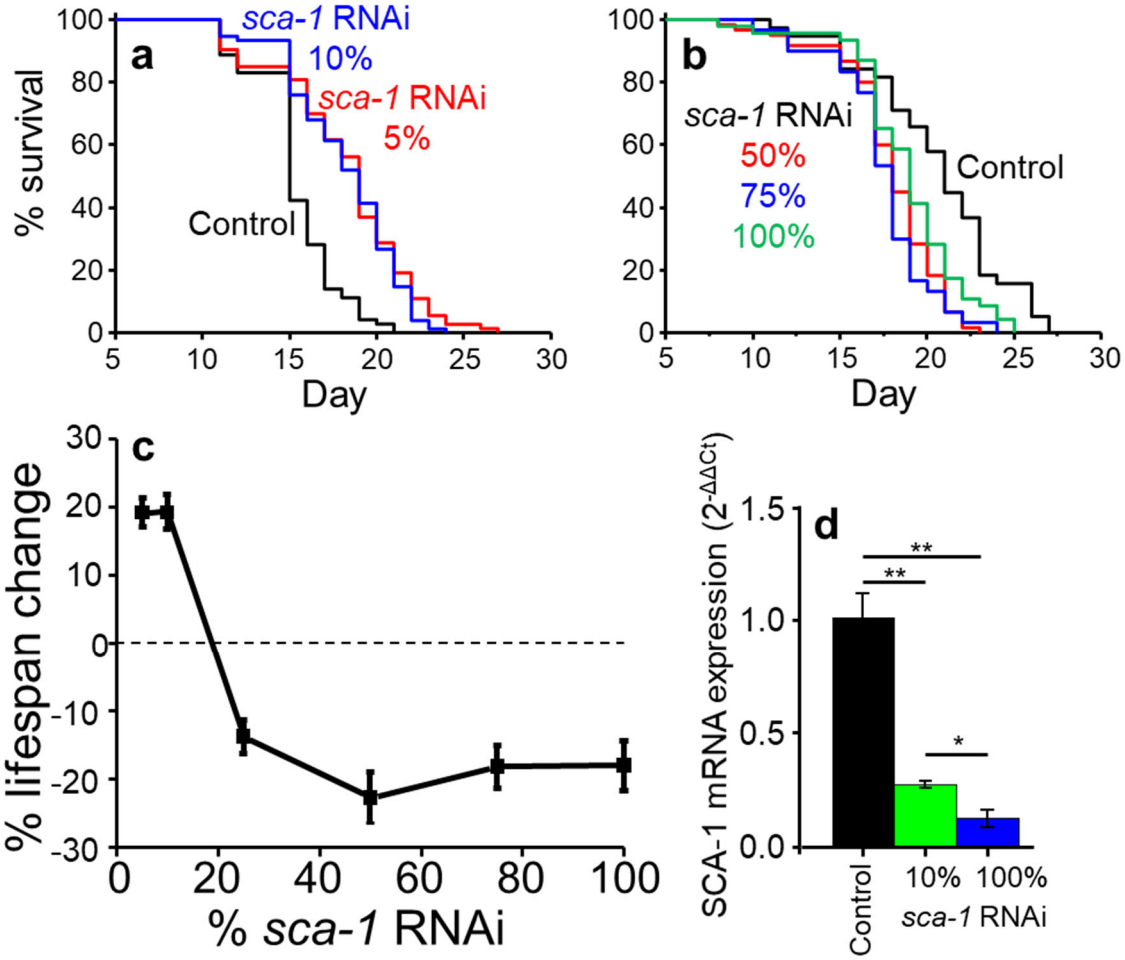

Figure 3. Effect of sca-1 RNAi on C. elegans lifespan. Panels a and b show representative survival plots corresponding to parallel lifespan trials (control vs drug) performed in N2 wild-type worms using several dilutions of *sca-1* RNAi. Panel a shows the effect of 5% and 10% *sca-1* RNAi, which both increase the lifespan, and panel b shows the effect of 50%, 75% and 100% *sca-1* RNAi, which all reduce the lifespan with respect to the N2 controls. The trials shown correspond to those marked in bold in Table S3. Panel c shows the mean changes in lifespan induced by the different dilutions (more details and statistics of the assays in Tables S1 and S3). Panel d shows the SCA-1 mRNA expression at day 5 of adult life in control worms or in worms treated with 10% or 100% *sca-1* RNAi from day 1 of adult life.

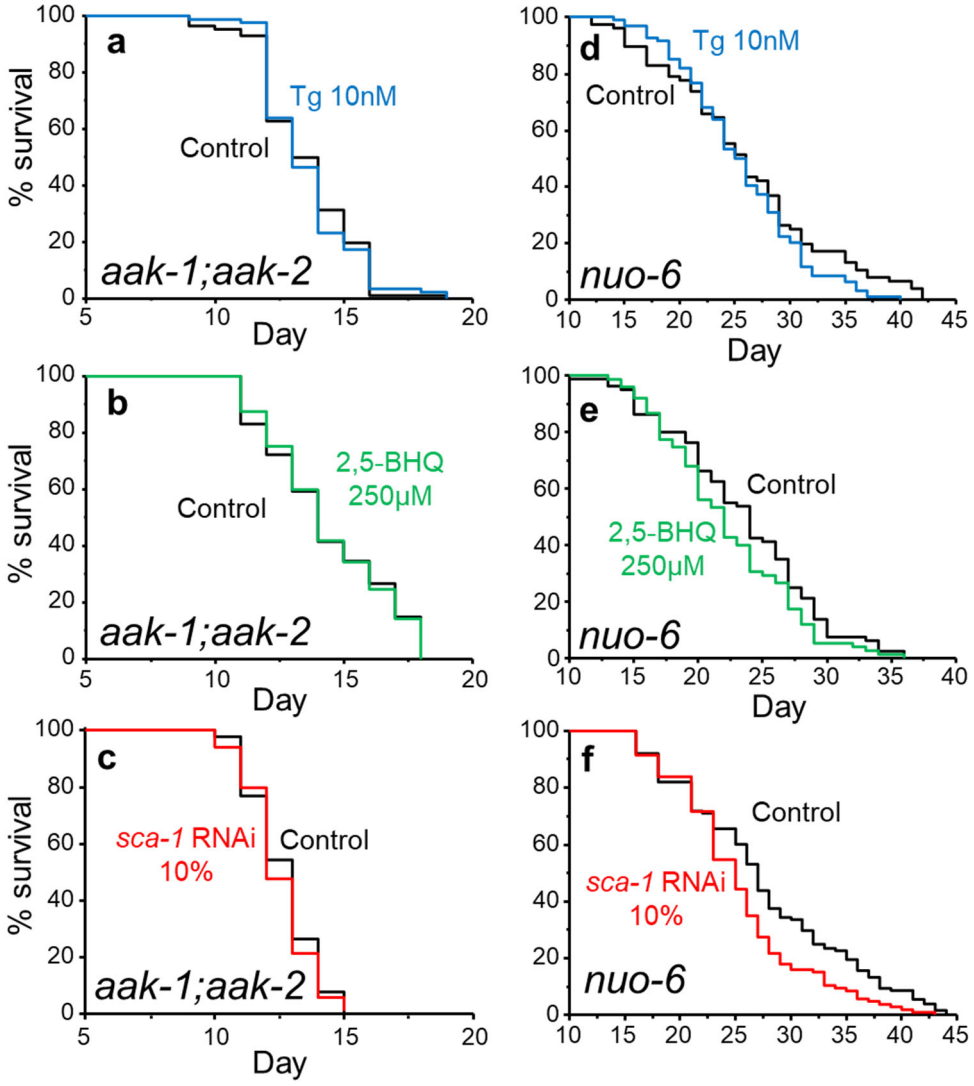

Figure 4. Effect of SERCA inhibition on the lifespan of *aak-1;aak-2* and *nuo-6* mutants. Panels show representative survival plots corresponding to parallel lifespan trials (control vs drug) performed in *aak-1;aak-2* mutants (panels a-c) or *nuo-6* mutants (panels d-f) using either 10nM thapsigargin (panels a,d), 250µM 2,5-BHQ (panels b,e) or 10% sca-1 RNAi (panels c,f). In each panel, the trace labelled "Control" was obtained with the corresponding mutant, and the other was obtained in the same mutant treated with the drug or *sca-1* RNAi from day 1 of adult life. The trials shown correspond to those marked in bold in Table S4 (more details and statistics of all the assays in Tables S1 and S4).

3.4 Effect of SERCA inhibitors on *C. elegans* AMPK or mitochondrial respiratory chain mutants.

We have then investigated the possible involvement of the AMP-activated kinase (AMPK) in the effect of the SERCA inhibitors. The *C. elegans* genome encodes two homologs of the α-catalytic subunits of mammalian AMPK, which are known as *aak-1* and *aak-2* (Sun et al., 2017). We have studied the effects of the SERCA inhibitors in the double *aak-1;aak-2* mutant

(Fig. 4, panels a-b, table S4a) and we found that they had no effect at all. Consistently, 10% sca-1 RNAi was unable to increase the lifespan of this mutant (Fig. 4, panel c). Therefore the increase in lifespan induced by SERCA inhibitors is somehow mediated by AMPK activity.

To explore the effect of mutations affecting the mitochondrial respiratory chain, we have used the *nuo-6* mutant, which has a mutation in a conserved subunit of mitochondrial complex I. The mutation reduces the function of complex I and results in low oxygen consumption, slow growth, slow behavior, and increased lifespan (Yang and Hekimi, 2010a). Fig. 4, panels d-f and table S4b show that neither SERCA inhibitors nor *sca-1* RNA-i produced lifespan extension at all in this mutant. In fact, most of the trials produced either not significant differences or even a decrease in lifespan. These results show that mitochondrial function is clearly involved in the effect of the SERCA inhibitors.

To exclude a possible interference in our results of the metabolism of SERCA inhibitors by E. coli bacteria, we have studied the effects of these compounds in wild-type worms fed with inactivated OP50. Fig. S1 and table S5 show that the results were similar to those obtained in the presence of live OP50. Thapsigargin and 2,5-BHQ increased lifespan by 7.5±3.2% and 18.8±2.5%, respectively.

3.5 Effect of SERCA inhibition on mutants of Ca^{2+} pathways.

One of the targets of the Ca^{2+} released from the ER is mitochondria, and the only Ca^{2+} channel known to transport Ca^{2+} through the inner mitochondrial membrane is the mitochondrial Ca^{2+} uniporter (MCU) (De Stefani et al., 2011). To explore the possible role of this channel in the mechanism of the effect of SERCA inhibition, we have studied the effect of *sca-1* RNAi in the mutant *mcu-1* strain (Xu and Chisholm, 2014), which harbor a large deletion in the pore region of the *mcu-1* gene, the worm orthologue of the MCU channel. We have to mention, however, that mitochondrial Ca^{2+} oscillations in pharynx muscle cells continue unchanged in the *mcu-1* mutant (Álvarez-Illera et al., 2020), indicating that there must be another independent Ca^{2+} pathway that mediates mitochondrial Ca^{2+} uptake in these mutants.

Fig. 5a and Table S6 show that *mcu-1* mutants have a nearly 10% increased lifespan with respect to the N2 wild-type worms. Addition of sca-1 RNAi (10% dilution) produced an increase in lifespan both in the N2 wild-type strain and in the *mcu-1* mutants, and the combination of *sca-1* RNAi and the *mcu-1* mutation produced an increase in lifespan which was significantly larger than those induced by *sca-1* RNAi or the *mcu-1* mutation alone, and almost additive, in all the three trials performed (see Table S6). This suggests that the MCU Ca^{2+} channel is not essential for the effect on lifespan of SERCA inhibition.

We have also studied the effect of *sca-1* RNAi on the *unc-68(r1161)* null mutant. UNC-68 is the only representative in *C. elegans* of the ryanodine receptor, one of the endoplasmic reticulum Ca^{2+} channels. Fig. 5b and table S7 show that *sca-1* RNAi increased the lifespan also in this mutant, but only by about 8%, about half the effect obtained in wild-type worms.

This suggests that ryanodine receptors may contribute in part to the increase in lifespan induced by sca-1 RNAi.

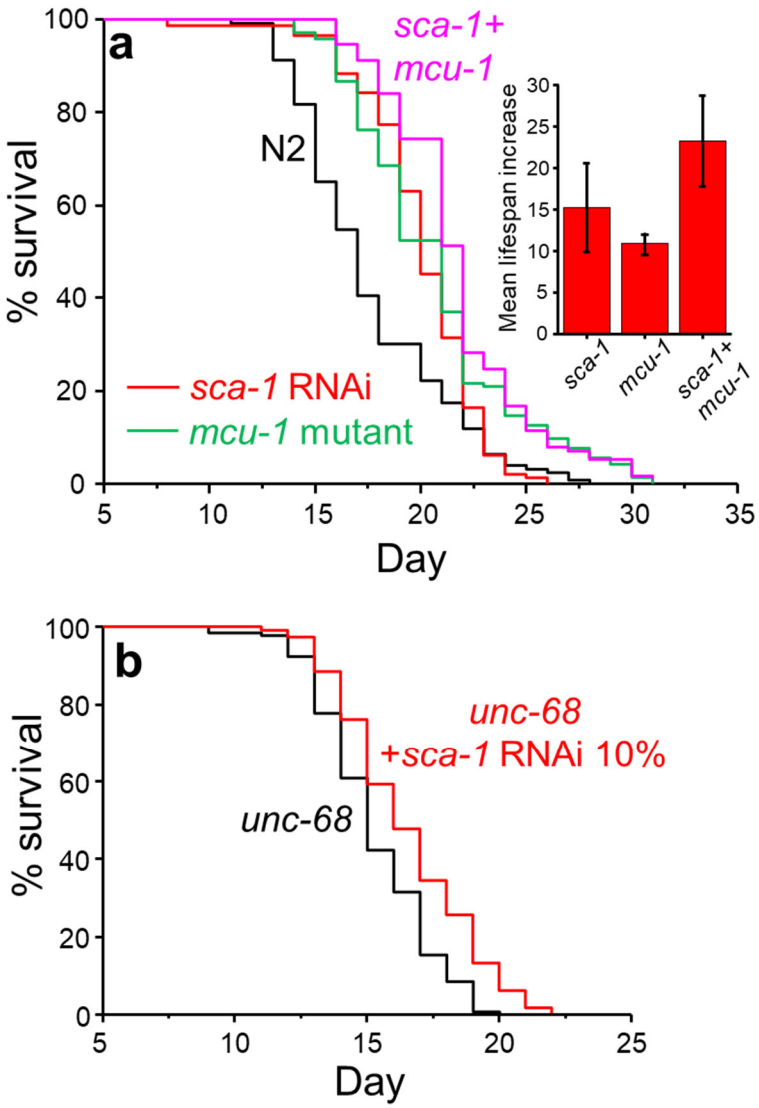

Fig. 5. Effect of *sca-1* RNAi on the lifespan of *mcu-1* and *unc-68* mutants. Panel a shows representative survival plots corresponding to parallel lifespan trials performed with N2 worms, N2 worms treated with 10% sca-1 RNAi, *mcu-1* mutants and *mcu-1* mutants treated with 10% sca-1 RNAi from day 1 of adult life. The trials shown correspond to those marked in bold in table S6. Panel b shows representative survival plots corresponding to parallel lifespan trials performed with *unc-68* mutants treated or not with 10% sca-1 RNAi from day 1 of adult life. The trials shown correspond to those marked in bold in table S7. More details and statistics of all the assays in Tables S1, S6 and S7.

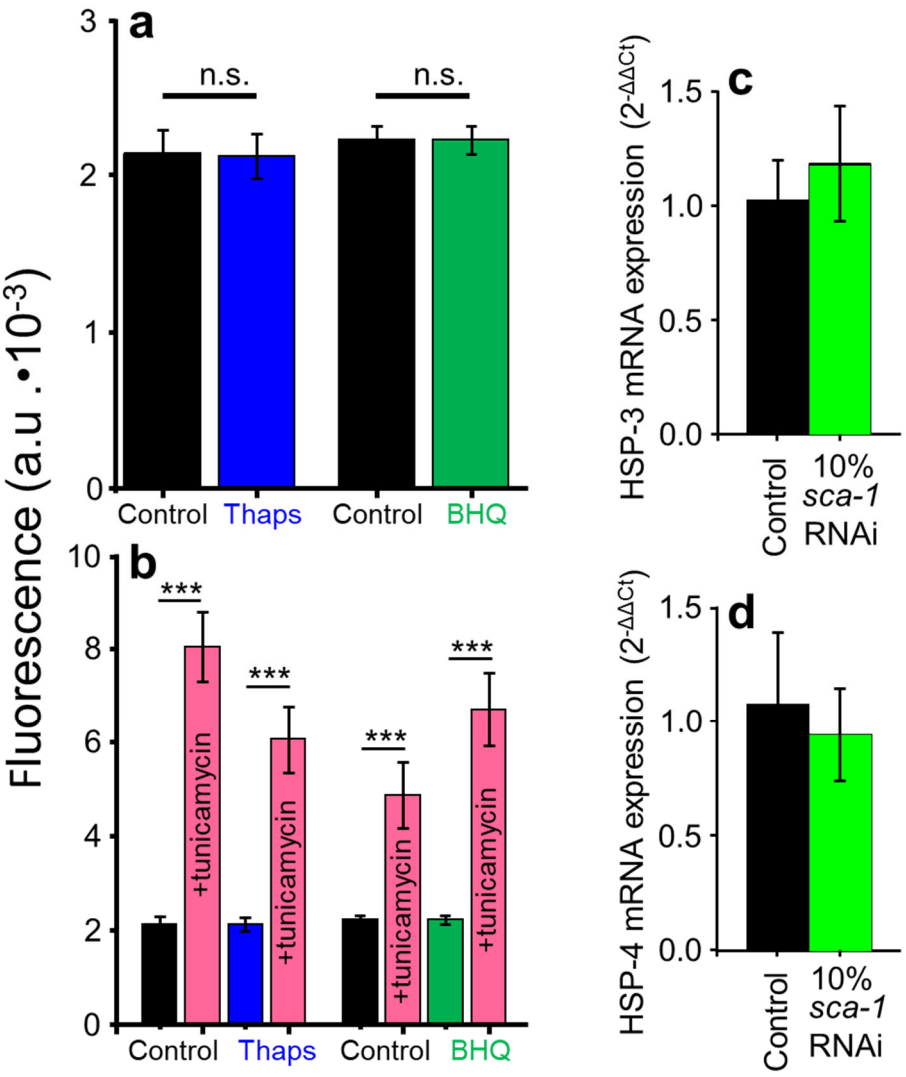

399

400 **Figure 6. Effect of SERCA inhibitors on ER stress.** Panels a and b show the mean
401 fluorescence obtained from SJ4005 (expressing *hsp-4*::GFP) worms after different
402 treatments. Panel a shows the effects of 3 days treatment with thapsigargin or 2,5-BHQ. Panel
403 b shows the effects of the same treatments either in the absence or in the presence of
404 tunicamycin. Controls were added the corresponding amount of DMSO. ***, $p<0.001$. Error
405 bars are s.e.m. (n=40-42 worms analyzed in each condition). Panels c and d show the effect
406 of *sca-1* RNAi on mRNA expression of HSP-3 and HSP-4 measured by RT-qPCR at day 5
407 of adult life. Bars show mean±s.e., n=3.

408

409 **3.6 Effect of SERCA inhibitors on ER stress.**

410 Finally, we have investigated the effects of the SERCA inhibition on ER stress in wild-type
411 worms. It is well know that thapsigargin is able to induce ER stress as a consequence of the
412 ER Ca^{2+} depletion (Foufelle and Fromenty, 2016). However, we wanted to know if the
413 submaximal concentrations of SERCA inhibitors used in our study were able to induce it in
414 the worms. To study ER stress, we have first used the SJ4005 strain, which contains a GFP

reporter transgene under the control of the *hsp-4* promoter. Induction of ER stress leads to a strong increase in GFP expression, reflecting the upregulation of the *hsp-4* gene. Fig. 6a and 6b show the mean worm fluorescence and Fig. S2 shows the fluorescence images. Fig. 6a shows that none of the compounds increased *hsp-4* expression. Fig. 6b shows the increase in fluorescence induced by incubation with tunicamycin in each of the conditions of Fig. 6a. In addition, we have also studied mRNA expression of two markers of ER stress, HSP-3 and HSP-4. Fig. 6c and 6d show that 10% *sca-1* RNAi did not increase mRNA expression of these markers. Our data therefore show that neither inhibition of SERCA by thapsigargin or 2,5-BHQ, at concentrations that increase *C. elegans* lifespan, nor decrease in mRNA expression by 10% *sca-1* RNAi, does not induce ER stress.

4. DISCUSSION

We have reported recently that submaximal concentrations of SERCA inhibitors increase the lifespan of *C. elegans* worms (García-Casas et al., 2018). The mechanism was not related with dietary restriction, as the SERCA inhibitors produced similar effects in the *eat-2* mutant, which has a defect in pharynx pumping that impairs feeding and has a longer lifespan as a consequence of the reduced food ingestion (Jia and Levine, 2007). We have used here *C. elegans* strains harboring mutations in several pathways known to be involved in the control of longevity, and we have looked for overlaps among the mechanisms activated by the SERCA inhibitors and the pathways inactivated in the mutants. In addition, we show that the effects of the SERCA inhibitors are not due to induction of ER stress at the concentrations used, and they are also independent on the *E. coli* metabolism of the drugs.

To inhibit SERCA in the worms, we have used the potent and specific inhibitor thapsigargin and the widely used compound 2,5-BHQ. SERCA (SCA-1 in *C. elegans*) is highly conserved between mammals and *C. elegans*, and SCA-1 shows about 70% amino acid identity and 80% similarity to the three human SERCA proteins. In particular, the amino acids present in the binding pocket for thapsigargin (Paula and Ball, 2004) are completely conserved in SCA-1 (Cho et al., 2000), and SCA-1 also conserves the two amino acids, Asp59 and Pro308, that make hydrogen bonding with the hydroxyl groups of 2,5-BHQ in human SERCA (Elam et al., 2011; Lape et al., 2008). In addition, thapsigargin has been shown before to produce the same effects in *C. elegans* that depletion of the SCA-1 gene (Zwaal et al., 2001). Similarly, in *C. elegans* models of neurodegeneration where thapsigargin behaves as a protective agent, the effect of thapsigargin is redundant with SCA-1 depletion with RNAi (Griffin et al., 2019). Therefore, there is evidence that thapsigargin inhibits SCA-1 in *C. elegans*. Regarding 2,5-BHQ, there is no direct evidence that it is inhibiting SERCA in the worms, but the conservation of the amino acids responsible for BHQ binding suggests that it should also be able to do it.

In addition, we have shown that partial inhibition of SCA-1 expression with submaximal concentrations of RNAi increased lifespan in the same way that SERCA inhibitors, while

larger concentrations of RNAi reduced lifespan. This provides further evidence that the increase in lifespan in all the cases is mediated by submaximal inhibition of SERCA.

Our results show that SERCA inhibitors were still able to increase longevity in *daf-2* (insulin/IGF-1 receptor) and *sir-2.1* (sirtuin 1 homolog) mutants nearly as much as in the wild-type worms (García-Casas et al., 2018). Therefore, the effect is not mediated by these pathways. Instead, the effect of the SERCA inhibitors was clearly blocked in *daf-15*/RAPTOR mutants and double *aak-1;aak-2* (AMPK α-subunits) mutants. Therefore, the effect requires the activity of both TORC1 and AMPK.

The effect of SERCA inhibition also disappeared in *nuo-6* mitochondrial respiratory chain complex I mutants. *nuo-6* mutants are defective in a subunit of complex I of the mitochondrial respiratory chain, and they have reduced mitochondrial function and display lower oxygen consumption, slow growth, slow movement, decreased ATP levels and a significant lifespan extension (Yang and Hekimi, 2010a, 2010b). They have also increased mitochondrial superoxide production, which is important for the increase in longevity (Yang and Hekimi, 2010b; Yee et al., 2014). In fact, an increase in lifespan is a common fact of many mild mitochondrial respiratory chain mutants (Senchuk et al., 2018) and ROS appear to play an important role in the increased longevity. When we use SERCA inhibitors or *sca-1* RNAi in *nuo-6* mutants, we see that not only do they not produce an increase in longevity, but they actually decrease the lifespan of the mutants. This suggests that the mechanism of the effect of SERCA inhibition overlaps completely with that induced by the mitochondrial defect, and the presence of intact mitochondria is essential for the effect on longevity of SERCA inhibition to be observed.

Regarding the *daf-16* mutant, we have seen that SERCA inhibitors produce some increase in lifespan, but clearly smaller than that obtained in the wild-type (García-Casas et al., 2018). Therefore, it is probably also involved in the effect of the SERCA inhibitors, or at least in part of it. The DAF-16 gene is placed at the crossroads of multiple signaling pathways and is modulated by the flow of the insulin-activated pathway and the AMPK, TOR and sirtuin pathways, among others (Lapierre and Hansen, 2012; Sun et al., 2017; Wang and Tissenbaum, 2006; Zhao and Wang, 2016). Therefore, if the TORC1 and AMPK were implicated in the effect, it is quite reasonable that DAF-16 was too. In addition, the involvement of DAF-16 is consistent with the fact that mitochondrial mutants, including *nuo-6*, show upregulation of DAF-16/FOXO target genes and that DAF-16 is required for the increased longevity of these mitochondrial mutants (Senchuk et al., 2018).

The connection between the effects of the SERCA inhibitors and the pathways involved must occur somehow through changes in Ca^{2+} signaling. Submaximal inhibition of the Ca^{2+} pump of the sarcoplasmic and endoplasmic reticulum should lead to a reduction in the level of Ca^{2+} in these compartments. The immediate consequence would be a decrease in the amount of Ca^{2+} released during cell stimulation, either through the inositol 1,4,5-trisphosphate receptor (IP_3R) or through the ryanodine receptor (RyR). Among many other functions, Ca^{2+} release from the endoplasmic reticulum is very important to activate mitochondrial metabolism. In the last few years, the importance of the close contacts between endoplasmic reticulum and

mitochondria, also known as mitochondria-associated ER membranes (MAMs), has been increasingly acknowledged. In fact, these ER-mitochondria contacts have been proposed to be signaling hubs with critical roles in the development of many diseases, including cancer, neurodegenerative diseases or aging (Gómez-Suaga et al., 2018; Kerkhofs et al., 2018; Moltedo et al., 2019). One of the proposed functions of these MAMs is the transfer of Ca^{2+} from ER to mitochondria via IP_3R in the ER, voltage-dependent anion channels (VDAC/porin) in the outer mitochondrial membrane and the mitochondrial Ca^{2+} uniporter (MCU) in the inner mitochondrial membrane. The large local accumulation of Ca^{2+} close to the IP_3R would be enough to activate the mitochondrial Ca^{2+} uniporter and allow a fast transfer of Ca^{2+} among the two organelles (Moltedo et al., 2019).

Of course, the route for mitochondrial Ca^{2+} entry plays an essential role in this mechanism. The MCU is the only channel known up to date to mediate mitochondrial Ca^{2+} uptake. However, it has been shown that knockout mice lacking MCU were viable and showed a very mild phenotype (Holmström et al., 2015; Pan et al., 2013). Similarly, a *C. elegans* strain with a large deletion in the MCU pore region (*mcu-1*) has a nearly normal phenotype with only minor defects in wound closure (Xu and Chisholm, 2014). And we have recently shown that mitochondrial Ca^{2+} oscillations in *C. elegans* pharynx are fully preserved in the *mcu-1* mutant (Álvarez-Illera et al., 2020), indicating that a different mitochondrial Ca^{2+} entry pathway must be present. In any case, we have tested here the effect of SERCA inhibition in the *mcu-1* mutants. Our results show first that the *mcu-1* mutant has a nearly 10% increase in lifespan with respect to the N2 wild-type worms. The origin of this increased longevity is obscure. Perhaps the absence of MCU could facilitate long-term survival by preventing mitochondrial Ca^{2+} overload under some stress conditions. In any case, *sca-1* RNAi (10% dilution) induced a significant further increase in longevity in the *mcu-1* mutants, indicating that the presence of MCU is not essential for the effect. This result certainly does not rule out that Ca^{2+} transfer from ER to mitochondria is important for the effect of SERCA inhibitors on longevity, since there must be an alternative pathway for Ca^{2+} entry into mitochondria.

Regarding the route for ER-Ca^{2+} release, the two main Ca^{2+} channels of the ER are IP_3R and RyR. IP_3R are very good candidates, because it is the ER Ca^{2+} channel that accumulates in the MAMs (Moltedo et al., 2019) and has been recently shown to promote aging via ER-mitochondria contacts (Ziegler et al., 2021). However, *C. elegans* null IP_3R (*itr-1*) mutants have severe limitations and cannot be used for lifespan studies (Dal Santo et al., 1999). We have studied instead mutants of the RyR and we have seen that sca-1 RNAi still increases longevity in this mutants, although the effect is only about half that obtained in the wild-type worms. This indicates that this ER Ca^{2+}-channels may contribute in part to the effect.

Whatever is the mechanism responsible for mitochondrial Ca^{2+} uptake, SERCA inhibitors or *sca-1* RNAi, by reducing the level of Ca^{2+} in the ER, would reduce the possibility that an excess Ca^{2+} transfer would lead under pathological conditions to mitochondrial Ca^{2+} overload and apoptosis. Moreover, on a more physiological basis, SERCA inhibitors should reduce the amount of Ca^{2+} transfer from ER to mitochondria and the subsequent activation of mitochondrial metabolism. The fact that the increase in lifespan induced by the SERCA inhibitors disappears in the *nuo-6* mitochondrial respiratory chain complex I mutant suggests

that these changes in ER-mitochondria Ca^{2+} transfer are important for the effect. The reduced respiratory chain electron flux in the *nuo-6* mutant reduces the mitochondrial membrane potential, which is the main driving force for mitochondrial Ca^{2+} uptake. Therefore, ER-mitochondria Ca^{2+} transfer must be already reduced in this mutant, explaining why the SERCA inhibitors do not produce any further effect.

The decrease in ER-mitochondria Ca^{2+} transfer should slow down mitochondrial metabolism and ATP production, increasing the AMP/ATP ratio and thus activating AMPK. The lack of effect of the SERCA inhibitors in the double *aak-1;aak2* mutant suggests that this mechanism is essential for the effect. This effect may seem contradictory with the recently reported AMPK-induced activation of the mitochondrial Ca^{2+} uniporter (Zhao et al., 2019). However, although this mechanism may serve to keep some mitochondrial Ca^{2+} uptake in the presence of a reduced ER [Ca^{2+}] release, it will operate only as long as AMPK is persistently activated by a decreased ER-mitochondria Ca^{2+} transfer. Activation of AMPK may increase lifespan by several mechanisms, but one of the key ones is the inhibition of TORC1 by several mechanisms, one of them by direct phosphorylation of *daf-15*/RAPTOR (Boutouja et al., 2019; Gwinn et al., 2008). The lack of effect of SERCA inhibitors in the *daf-15* mutant suggests that this point is also essential. Thus, in the *daf-15* mutant, TORC1 signaling is already reduced, lifespan has been already increased and the SERCA inhibitors cannot produce any further effect.

In conclusion, our results suggest that the increase in lifespan induced by SERCA inhibitors is mediated by a reduced ER-mitochondria Ca^{2+} transfer that would activate AMPK and inhibit TORC1. This would increase survival by several mechanisms, including activation of autophagy and improved energy homeostasis. DAF-16 may also be involved in some degree, as both AMPK and TORC1 are known to modulate it (Sun et al., 2017). Fig. 7 shows a cartoon explaining this mechanism.

Consistently with this model, low concentrations of SERCA inhibitors have been shown before to have a protective effect against neurodegeneration, both in neuronal cell cultures (Lampe et al., 1995) and in *C. elegans* models of neurodegeneration (Betzer and Jensen, 2018; Griffin et al., 2019). Instead, high thapsigargin concentrations increase neurodegeneration in other *C. elegans* models (Aggad et al., 2014; Xu et al., 2001). These data have been interpreted to suggest a role for ER [Ca^{2+}] release also in the process of neurodegeneration.

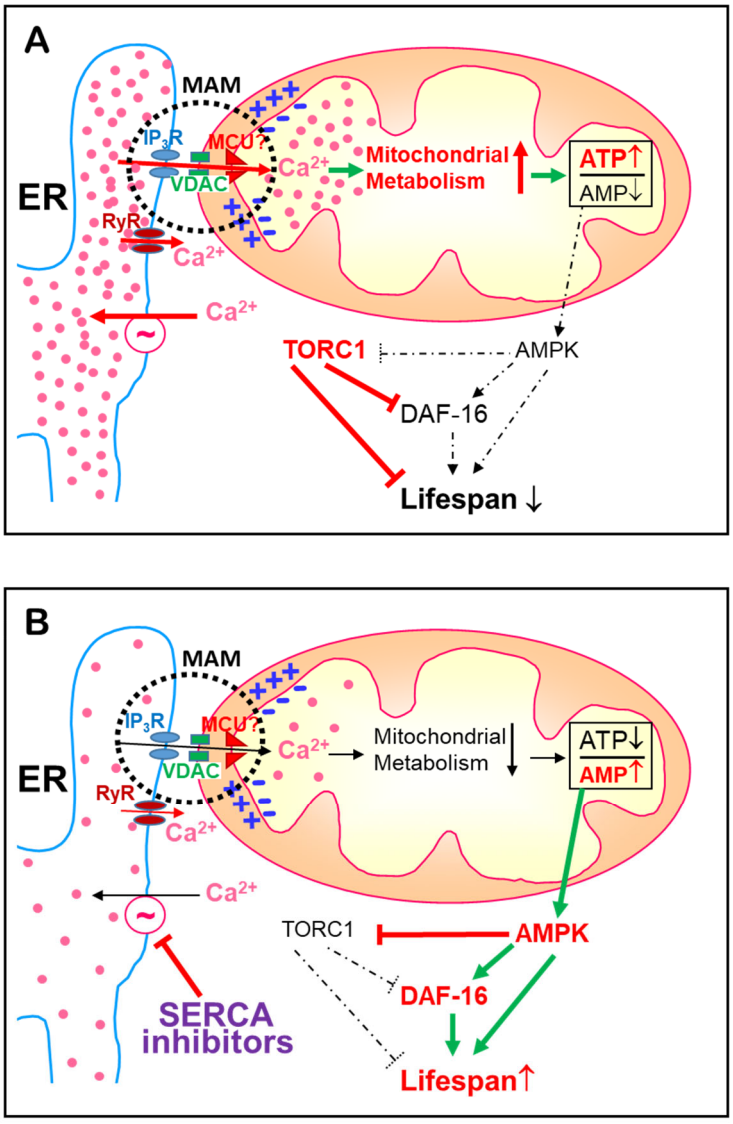

569

570 **Figure 7. Cartoon showing the proposed mechanism for the effect of the SERCA**
571 **inhibitors.** Ca^{2+} transfer from ER to mitochondria takes place in the MAMs, where IP_3R in
572 the ER membrane, VDAC porins in the outer mitochondrial membrane and MCU channels
573 in the inner mitochondrial membrane create a Ca^{2+} pathway between both organelles. RyR
574 also contribute to release Ca^{2+} close to mitochondria. In panel A, under control conditions,
575 Ca^{2+} transfer from ER to mitochondria increases mitochondrial metabolism and ATP
576 production. The increase in the ATP/AMP ratio inhibits AMPK, activating TORC1, which
577 has a negative impact on lifespan, in part via inhibition of DAF-16. In panel B, in the presence
578 of the SERCA inhibitors, the decrease in the ER Ca^{2+} content reduces ER to mitochondria
579 Ca^{2+} transfer. Mitochondrial metabolism is reduced and the ATP/AMP ratio decreases. AMP
580 increase leads to activation of AMPK, inhibition of TORC1 and increase in lifespan, in part
581 via DAF-16 activation.

582

583

DECLARATION OF COMPETING INTEREST

The authors declare no conflicts of interest.

AUTHOR CONTRIBUTIONS: MM and JA designed the project. PG-C and PA-I performed most of the experiments. JA wrote the manuscript and RIF and MM helped in discussing and editing the manuscript. All authors read and approved the final manuscript.

FUNDING: This research was funded by the Spanish Ministry of Economy, Industry and Competitiveness, Government of Spain (Ministerio de Economía, Industria y Competitividad, Gobierno de España) to MM and JA, grant number BFU2017-83509-R, project co-financed by the European Union through the European Regional Development Fund. It was also funded by a grant from the Ministry of Education, Board of Castilla y León (Consejería de Educación, Junta de Castilla y León; VA011G18) to JA. PG-C had a FPI fellowship from Ministry of Economy, Industry and Competitiveness.

ACKNOWLEDGMENTS: Some *C. elegans* strains were provided by the Caenorhabditis Genetics Center (CGC), which is funded by NIH Office of Research Infrastructure Programs (P40 OD010440). We thank Dr. Malene Hansen, Sanford Burnham Prebys Medical Discovery Institute, La Jolla, USA, for providing us with the strain SJ4005.

DATA AVAILABILITY STATEMENT

The raw data supporting the conclusions of this manuscript will be made available by the authors, without undue reservation, to any qualified researcher

SUPPLEMENTARY MATERIALS: Supplementary materials can be found below.

615

616 **REFERENCES**

617 Aggad, D., Vérièpe, J., Tauffenberger, A., Parker, J.A., 2014. TDP-43 toxicity proceeds via
618 calcium dysregulation and necrosis in aging Caenorhabditis elegans motor neurons. J.
619 Neurosci. 34, 12093–12103. https://doi.org/10.1523/JNEUROSCI.2495-13.2014

620 Ahumada-Castro, U., Silva-Pavez, E., Lovy, A., Pardo, E., Molgó, J., Cárdenas, C., 2019.
621 MTOR-independent autophagy induced by interrupted endoplasmic reticulum-
622 mitochondrial Ca $^{2+}$ communication: a dead end in cancer cells. Autophagy 15, 358–
623 361. https://doi.org/10.1080/15548627.2018.1537769

624 Álvarez-Illera, P., García-Casas, P., Fonteriz, R.I., Montero, M., Alvarez, J., 2020.
625 Mitochondrial Ca2+ dynamics in MCU knockout C. Elegans worms. Int. J. Mol. Sci.
626 21, 1–11. https://doi.org/10.3390/ijms21228622

627 Alvarez-Illera, P., Sanchez-Blanco, A., Lopez-Burillo, S., Fonteriz, R.I., Alvarez, J.,
628 Montero, M., 2016. Long-term monitoring of Ca2+ dynamics in C. elegans pharynx:
629 an in vivo energy balance sensor. Oncotarget 7, 67732–47.
630 https://doi.org/10.18632/oncotarget.12177

631 Arias-del-Val, J., Santo-Domingo, J., García-Casas, P., Alvarez-Illera, P., Núñez Galindo,
632 A., Wiederkehr, A., Fonteriz, R.I., Montero, M., Alvarez, J., 2019. Regulation of
633 inositol 1,4,5-trisphosphate-induced Ca2+ release from the endoplasmic reticulum by
634 AMP-activated kinase modulators. Cell Calcium 77, 68–76.
635 https://doi.org/10.1016/j.ceca.2018.12.004

636 Betzer, C., Jensen, P.H., 2018. Reduced Cytosolic Calcium as an Early Decisive Cellular
637 State in Parkinson's Disease and Synucleinopathies. Front. Neurosci. 12, 819.
638 https://doi.org/10.3389/fnins.2018.00819

639 Blackwell, T.K., Sewell, A.K., Wu, Z., Han, M., 2019. TOR Signaling in Caenorhabditis
640 elegans Development, Metabolism, and Aging . Genetics 213, 329–360.
641 https://doi.org/10.1534/genetics.119.302504

642 Bootman, M.D., Chehab, T., Bultynck, G., Parys, J.B., Rietdorf, K., 2018. The regulation
643 of autophagy by calcium signals: Do we have a consensus? Cell Calcium 70, 32–46.
644 https://doi.org/https://doi.org/10.1016/j.ceca.2017.08.005

645 Boutouja, F., Stiehm, C.M., Platta, H.W., 2019. mTOR: A Cellular Regulator Interface in
646 Health and Disease. Cells 8, 18. https://doi.org/10.3390/cells8010018

647 Carroll, B., Korolchuk, V.I., Sarkar, S., 2015. Amino acids and autophagy: cross-talk and
648 co-operation to control cellular homeostasis. Amino Acids 47, 2065–2088.
649 https://doi.org/10.1007/s00726-014-1775-2

650 Castillo-Quan, J.I., Kinghorn, K.J., Bjedov, I., 2015. Genetics and Pharmacology of
651 Longevity, in: Advances in Genetics. pp. 1–101.
652 https://doi.org/10.1016/bs.adgen.2015.06.002

653 Chauhan, A.S., Liu, X., Jing, J., Lee, H., Yadav, R.K., Liu, J., Zhou, Y., Gan, B., 2019.
654 STIM2 interacts with AMPK and regulates calcium-induced AMPK activation.
655 FASEB J. 33, 2957–2970. https://doi.org/10.1096/fj.201801225R

656 Cho, J.H., Bandyopadhyay, J., Lee, J., Park, C.S., Ahnn, J., 2000. Two isoforms of
657 sarco/endoplasmic reticulum calcium ATPase (SERCA) are essential in
658 Caenorhabditis elegans. Gene 261, 211–219. https://doi.org/10.1016/S0378-
659 1119(00)00536-9

660 Dal Santo, P., Logan, M.A., Chisholm, A.D., Jorgensen, E.M., 1999. The inositol
661 trisphosphate receptor regulates a 50-second behavioral rhythm in C. elegans. Cell 98,
662 757–767. https://doi.org/10.1016/S0092-8674(00)81510-X

663 De Stefani, D., Raffaello, A., Teardo, E., Szabó, I., Rizzuto, R., 2011. A forty-kilodalton
664 protein of the inner membrane is the mitochondrial calcium uniporter. Nature 476,
665 336–340. https://doi.org/10.1038/nature10230

666 Dorman, J.B., Albinder, B., Shroyer, T., Kenyon, C., 1995. The age-1 and daf-2 genes
667 function in a common pathway to control the lifespan of Caenorhabditis elegans.
668 Genetics 141, 1399–406.

669 Elam, C., Lape, M., Deye, J., Zultowsky, J., Stanton, D.T., Paula, S., 2011. Discovery of
670 novel SERCA inhibitors by virtual screening of a large compound library. Eur. J. Med.
671 Chem. 46, 1512–1523. https://doi.org/10.1016/j.ejmech.2011.01.069

672 Foufelle, F., Fromenty, B., 2016. Role of endoplasmic reticulum stress in drug-induced
673 toxicity. Pharmacol. Res. Perspect. 4, e00211. https://doi.org/10.1002/prp2.211

674 García-Casas, P., Arias-del-Val, J., Alvarez-Illera, P., Fonteriz, R.I., Montero, M., Alvarez,
675 J., 2018. Inhibition of Sarco-Endoplasmic Reticulum Ca2+ ATPase Extends the
676 Lifespan in C. elegans Worms. Front. Pharmacol. 9, 669.
677 https://doi.org/10.3389/fphar.2018.00669

678 Gómez-Suaga, P., Bravo-San Pedro, J.M., González-Polo, R.A., Fuentes, J.M., Niso-
679 Santano, M., 2018. ER-mitochondria signaling in Parkinson's disease. Cell Death Dis.
680 9, 337. https://doi.org/10.1038/s41419-017-0079-3

681 Gomez-Suaga, P., Paillusson, S., Miller, C.C.J., 2017. ER-mitochondria signaling regulates
682 autophagy. Autophagy 13, 1250–1251.
683 https://doi.org/10.1080/15548627.2017.1317913

684 Griffin, E.F., Scopel, S.E., Stephen, C.A., Holzhauer, A.C., Vaji, M.A., Tuckey, R.A.,
685 Berkowitz, L.A., Caldwell, K.A., Caldwell, G.A., 2019. ApoE-associated modulation

of neuroprotection from Aβ-mediated neurodegeneration in transgenic Caenorhabditis elegans. Dis. Model. Mech. 12, dmm037218. https://doi.org/10.1242/dmm.037218

Gwinn, D.M., Shackelford, D.B., Egan, D.F., Mihaylova, M.M., Mery, A., Vasquez, D.S., Turk, B.E., Shaw, R.J., 2008. AMPK Phosphorylation of Raptor Mediates a Metabolic Checkpoint. Mol. Cell 30, 214–226. https://doi.org/10.1016/j.molcel.2008.03.003

Holmström, K.M., Pan, X., Liu, J.C., Menazza, S., Liu, J., Nguyen, T.T., Pan, H., Parks, R.J., Anderson, S., Noguchi, A., Springer, D., Murphy, E., Finkel, T., 2015. Assessment of cardiac function in mice lacking the mitochondrial calcium uniporter. J. Mol. Cell. Cardiol. 85, 178–82. https://doi.org/10.1016/j.yjmcc.2015.05.022

Ito, N., Ruegg, U.T., Kudo, A., Miyagoe-Suzuki, Y., Takeda, S., 2013. Activation of calcium signaling through Trpv1 by nNOS and peroxynitrite as a key trigger of skeletal muscle hypertrophy. Nat Med 19, 101–106. https://doi.org/10.1038/nm.3019

Jeon, S.M., 2016. Regulation and function of AMPK in physiology and diseases. Exp Mol Med 48, e245. https://doi.org/10.1038/emm.2016.81

Jia, K., Chen, D., Riddle, D.L., 2004. The TOR pathway interacts with the insulin signaling pathway to regulate C. elegans larval development, metabolism and life span. Development 131, 3897–3906. https://doi.org/10.1242/dev.01255

Jia, K., Levine, B., 2007. Autophagy is Required for Dietary Restriction-Mediated Life Span Extension in *C. elegans*. Autophagy 3, 597–599. https://doi.org/10.4161/auto.4989

Kapahi, P., Chen, D., Rogers, A.N., Katewa, S.D., Li, P.W.-L., Thomas, E.L., Kockel, L., 2010. With TOR, less is more: a key role for the conserved nutrient-sensing TOR pathway in aging. Cell Metab. 11, 453–65. https://doi.org/10.1016/j.cmet.2010.05.001

Kapulkin, W.J., Kapulkin, V., Hiester, B.G., Link, C.D., 2005. Compensatory regulation among ER chaperones in C. elegans. FEBS Lett. 579, 3063–3068. https://doi.org/10.1016/j.febslet.2005.04.062

Kenyon, C., Chang, J., Gensch, E., Rudner, A., Tabtiang, R., 1993. A C. elegans mutant that lives twice as long as wild type. Nature 366, 461–464. https://doi.org/10.1038/366461a0

Kerkhofs, M., Bittremieux, M., Morciano, G., Giorgi, C., Pinton, P., Parys, J.B., Bultynck, G., 2018. Emerging molecular mechanisms in chemotherapy: Ca2+ signaling at the mitochondria-associated endoplasmic reticulum membranes. Cell Death Dis. 9, 334. https://doi.org/10.1038/s41419-017-0179-0

Kozlowski, L., Garvis, S., Bedet, C., Palladino, F., 2014. The Caenorhabditis elegans HP1 family protein HPL-2 maintains ER homeostasis through the UPR and hormesis. Proc. Natl. Acad. Sci. U. S. A. 111, 5956–5961. https://doi.org/10.1073/pnas.1321698111

722 Lampe, P.A., Cornbrooks, E.B., Juhasz, A., Johnson, E.M., Franklin, J.L., 1995.
723 Suppression of programmed neuronal death by a thapsigargin-induced Ca2+ influx. J.
724 Neurobiol. 26, 205–212. https://doi.org/10.1002/neu.480260205

725 Lape, M., Elam, C., Versluis, M., Kempton, R., Paula, S., 2008. Molecular determinants of
726 sarco/endoplasmic reticulum calcium ATPase inhibition by hydroquinone-based
727 compounds. Proteins 70, 639–649. https://doi.org/10.1002/prot.21542

728 Lapierre, L.R., Hansen, M., 2012. Lessons from C. elegans: signaling pathways for
729 longevity. Trends Endocrinol. Metab. 23, 637–644.
730 https://doi.org/10.1016/j.tem.2012.07.007

731 López-Otín, C., Blasco, M.A., Partridge, L., Serrano, M., Kroemer, G., 2013. The
732 hallmarks of aging. Cell 153, 1194–1217. https://doi.org/10.1016/j.cell.2013.05.039

733 MacMillan, D., Currie, S., Bradley, K.N., Muir, T.C., McCarron, J.G., 2005. In smooth
734 muscle, FK506-binding protein modulates IP3 receptor-evoked Ca2+ release by
735 mTOR and calcineurin. J Cell Sci 118, 5443–5451. https://doi.org/10.1242/jcs.02657

736 Moltedo, O., Remondelli, P., Amodio, G., 2019. The Mitochondria-Endoplasmic Reticulum
737 Contacts and Their Critical Role in Aging and Age-Associated Diseases. Front. Cell
738 Dev. Biol. 7, 172. https://doi.org/10.3389/fcell.2019.00172

739 Morissette, M.P., Susser, S.E., Stammers, A.N., Moffatt, T.L., Wigle, J.T., Wigle, T.J.,
740 Netticadan, T., Premecz, S., Jassal, D.S., O'Hara, K.A., Duhamel, T.A., 2019.
741 Exercise-induced increases in the expression and activity of cardiac sarcoplasmic
742 reticulum calcium ATPase 2 is attenuated in AMPKα 2 kinase-dead mice. Can. J.
743 Physiol. Pharmacol. 97, 786–795. https://doi.org/10.1139/cjpp-2018-0737

744 Mukhopadhyay, A., Oh, S.W., Tissenbaum, H.A., 2006. Worming pathways to and from
745 DAF-16/FOXO. Exp. Gerontol. 41, 928–34.
746 https://doi.org/10.1016/j.exger.2006.05.020

747 Nelson, M.E., Parker, B.L., Burchfield, J.G., Hoffman, N.J., Needham, E.J., Cooke, K.C.,
748 Naim, T., Sylow, L., Ling, N.X., Francis, D., Norris, D.M., Chaudhuri, R., Oakhill,
749 J.S., Richter, E.A., Lynch, G.S., Stöckli, J., James, D.E., 2019. Phosphoproteomics
750 reveals conserved exercise-stimulated signaling and AMPK regulation of store-
751 operated calcium entry. EMBO J. e102578. https://doi.org/10.15252/embj.2019102578

752 Ogawa, A., Firth, A.L., Smith, K.A., Maliakal, M. V., Yuan, J.X.-J., 2012. PDGF enhances
753 store-operated Ca2+ entry by upregulating STIM1/Orai1 via activation of Akt/mTOR
754 in human pulmonary arterial smooth muscle cells. Am. J. Physiol. Physiol. 302, C405–
755 C411. https://doi.org/10.1152/ajpcell.00337.2011

756 Pan, X., Liu, J., Nguyen, T., Liu, C., Sun, J., Teng, Y., Fergusson, M.M., Rovira, I.I., Allen,
757 M., Springer, D.A., Aponte, A.M., Gucek, M., Balaban, R.S., Murphy, E., Finkel, T.,
758 2013. The Physiological Role of Mitochondrial Calcium Revealed by Mice Lacking

759 the Mitochondrial Calcium Uniporter. Nat. Cell Biol. 15, 1464–1472.
760 https://doi.org/10.1038/ncb2868

761 Paula, S., Ball, W.J., 2004. Molecular determinants of thapsigargin binding by SERCA
762 Ca2+-ATPase: a computational docking study. Proteins 56, 595–606.
763 https://doi.org/10.1002/prot.20105

764 Peng, H., Liu, J., Sun, Q., Chen, R., Wang, Y., Duan, J., Li, C., Li, B., Jing, Y., Chen, X.,
765 Mao, Q., Xu, K.-F., Walker, C.L., Li, J., Wang, J., Zhang, H., 2013. mTORC1
766 enhancement of STIM1-mediated store-operated Ca2+ entry constrains tuberous
767 sclerosis complex-related tumor development. Oncogene 32, 4702–4711.
768 https://doi.org/10.1038/onc.2012.481

769 Régimbald-Dumas, Y., Frégeau, M.-O., Guillemette, G., 2011. Mammalian target of
770 rapamycin (mTOR) phosphorylates inositol 1,4,5-trisphosphate receptor type 2 and
771 increases its Ca2+ release activity. Cell. Signal. 23, 71–79.
772 https://doi.org/10.1016/j.cellsig.2010.08.005

773 Riera, C.E., Merkwirth, C., De Magalhaes Filho, C.D., Dillin, A., 2016. Signaling
774 Networks Determining Life Span. Annu. Rev. Biochem. 85, 35–64.
775 https://doi.org/10.1146/annurev-biochem-060815-014451

776 Senchuk, M.M., Dues, D.J., Schaar, C.E., Johnson, B.K., Madaj, Z.B., Bowman, M.J.,
777 Winn, M.E., Van Raamsdonk, J.M., 2018. Activation of DAF-16/FOXO by reactive
778 oxygen species contributes to longevity in long-lived mitochondrial mutants in
779 Caenorhabditis elegans. PLoS Genet. 14, e1007268.
780 https://doi.org/10.1371/journal.pgen.1007268

781 Stiernagle, T., 2006. Maintenance of *C. elegans* (February 11, 2006), WormBook, ed. C.
782 elegans Res. Community, Wormb. 1–11. https://doi.org/10.1895/wormbook.1.101.1

783 Sun, X., Chen, W.-D., Wang, Y.-D., 2017. DAF-16/FOXO Transcription Factor in Aging
784 and Longevity. Front. Pharmacol. 8, 548. https://doi.org/10.3389/fphar.2017.00548

785 Wang, Y., Hekimi, S., 2015. Mitochondrial dysfunction and longevity in animals:
786 Untangling the knot. Science (80-.). 350, 1204–1207.
787 https://doi.org/10.1126/science.aac4357

788 Wang, Y., Tissenbaum, H.A., 2006. Overlapping and distinct functions for a
789 Caenorhabditis elegans SIR2 and DAF-16/FOXO. Mech. Ageing Dev. 127, 48–56.
790 https://doi.org/10.1016/j.mad.2005.09.005

791 Woods, A., Dickerson, K., Heath, R., Hong, S.P., Momcilovic, M., Johnstone, S.R.,
792 Carlson, M., Carling, D., 2005. Ca2+/calmodulin-dependent protein kinase kinase-beta
793 acts upstream of AMP-activated protein kinase in mammalian cells. Cell Metab 2, 21–
794 33. https://doi.org/10.1016/j.cmet.2005.06.005

795 Xu, K., Tavernarakis, N., Driscoll, M., 2001. Necrotic cell death in C. elegans requires the
796 function of calreticulin and regulators of Ca2+ release from the endoplasmic
797 reticulum. Neuron 31, 957–971. https://doi.org/10.1016/S0896-6273(01)00432-9

798 Xu, S., Chisholm, A.D., 2014. C.elegans epidermal wounding induces a mitochondrial ROS
799 burst that promotes wound repair. Dev. Cell 31, 48–60.
800 https://doi.org/10.1016/j.devcel.2014.08.002

801 Yang, W., Hekimi, S., 2010a. Two modes of mitochondrial dysfunction lead independently
802 to lifespan extension in Caenorhabditis elegans. Aging Cell 9, 433–447.
803 https://doi.org/10.1111/j.1474-9726.2010.00571.x

804 Yang, W., Hekimi, S., 2010b. A mitochondrial superoxide signal triggers increased
805 longevity in caenorhabditis elegans. PLoS Biol. 8, e1000556.
806 https://doi.org/10.1371/journal.pbio.1000556

807 Yavari, A., Bellahcene, M., Bucchi, A., Sirenko, S., Pinter, K., Herring, N., Jung, J.J.,
808 Tarasov, K. V., Sharpe, E.J., Wolfien, M., Czibik, G., Steeples, V., Ghaffari, S.,
809 Nguyen, C., Stockenhuber, A., Clair, J.R. St., Rimmbach, C., Okamoto, Y., Yang, D.,
810 Wang, M., Ziman, B.D., Moen, J.M., Riordon, D.R., Ramirez, C., Paina, M., Lee, J.,
811 Zhang, J., Ahmet, I., Matt, M.G., Tarasova, Y.S., Baban, D., Sahgal, N., Lockstone,
812 H., Puliyadi, R., de Bono, J., Siggs, O.M., Gomes, J., Muskett, H., Maguire, M.L.,
813 Beglov, Y., Kelly, M., dos Santos, P.P.N., Bright, N.J., Woods, A., Gehmlich, K.,
814 Isackson, H., Douglas, G., Ferguson, D.J.P., Schneider, J.E., Tinker, A., Wolkenhauer,
815 O., Channon, K.M., Cornall, R.J., Sternick, E.B., Paterson, D.J., Redwood, C.S.,
816 Carling, D., Proenza, C., David, R., Baruscotti, M., DiFrancesco, D., Lakatta, E.G.,
817 Watkins, H., Ashrafian, H., 2017. Mammalian γ2 AMPK regulates intrinsic heart rate.
818 Nat. Commun. 8, 1258. https://doi.org/10.1038/s41467-017-01342-5

819 Yee, C., Yang, W., Hekimi, S., 2014. The intrinsic apoptosis pathway mediates the pro-
820 longevity response to mitochondrial ROS in C elegans. Cell 157, 897–909.
821 https://doi.org/10.1016/j.cell.2014.02.055

822 Zhao, H., Li, Teng, Wang, K., Zhao, F., Chen, J., Xu, G., Zhao, J., Li, Ting, Chen, L., Li,
823 L., Xia, Q., Zhou, T., Li, H.-Y., Li, A.-L., Finkel, T., Zhang, X.-M., Pan, X., 2019.
824 AMPK-mediated activation of MCU stimulates mitochondrial Ca2+ entry to promote
825 mitotic progression. Nat. Cell Biol. 21, 476–486. https://doi.org/10.1038/s41556-019-
826 0296-3

827 Zhao, L., Wang, J., 2016. Uncovering the mechanisms of Caenorhabditis elegans ageing
828 from global quantification of the underlying landscape. J. R. Soc. Interface 13,
829 20160421. https://doi.org/10.1098/rsif.2016.0421

830 Ziegler, D. V., Vindrieux, D., Goehrig, D., Jaber, S., Collin, G., Griveau, A., Wiel, C.,
831 Bendridi, N., Djebali, S., Farfariello, V., Prevarskaya, N., Payen, L., Marvel, J.,
832 Aubert, S., Flaman, J.M., Rieusset, J., Martin, N., Bernard, D., 2021. Calcium channel

ITPR2 and mitochondria–ER contacts promote cellular senescence and aging. Nat. Commun. 12, 720. https://doi.org/10.1038/s41467-021-20993-z

Zwaal, R.R., Van Baelen, K., Groenen, J.T., van Geel, A., Rottiers, V., Kaletta, T., Dode, L., Raeymaekers, L., Wuytack, F., Bogaert, T., 2001. The sarco-endoplasmic reticulum Ca2+ ATPase is required for development and muscle function in *Caenorhabditis elegans*. J. Biol. Chem. 276, 43557–63. https://doi.org/10.1074/jbc.M104693200

FIGURE LEGENDS

Figure 1. Effect of SERCA inhibitors on the lifespan of *daf-2*, *daf-16* and *sir-2.*1 mutants. Panels show representative survival plots corresponding to parallel lifespan trials (control vs drug) performed in *daf-2* mutants (panels a-b), *daf-16* mutants (panels c-d) and sir-2.1 mutants (panels e-f) using either 10nM thapsigargin (panels a,c,e) or 250μM 2,5-BHQ (panels b,d,f). In each panel, the trace labelled "Control" was obtained with the corresponding mutant, and the other was obtained in the same mutant treated with the indicated drug from day 1 of adult life. The trials shown correspond to those marked in bold in Table S1 (more details and statistics of all the assays in Table S1).

Figure 2. Effect of SERCA inhibitors on the lifespan of *daf-15/unc-24* and *rsks-1* mutants. Panels show representative survival plots corresponding to parallel lifespan trials (control vs drug) performed in *daf-15/unc-24* mutants (panels a-b) and *rsks-1* mutants (panels c-d) using either 10nM thapsigargin (panels a,c) or 250μM 2,5-BHQ (panels b,d). In each panel, the trace labelled "Control" was obtained with the corresponding mutant, and the other was obtained in the same mutant treated with the indicated drug from day 1 of adult life. The trials shown correspond to those marked in bold in Table S2 (more details and statistics of all the assays in Tables S1 and S2).

Figure 3. Effect of sca-1 RNAi on C. elegans lifespan. Panels a and b show representative survival plots corresponding to parallel lifespan trials (control vs drug) performed in N2 wild-type worms using several dilutions of *sca-1* RNAi. Panel a shows the effect of 5% and 10% *sca-1* RNAi, which both increase the lifespan, and panel b shows the effect of 50%, 75% and 100% *sca-1* RNAi, which all reduce the lifespan with respect to the N2 controls. The trials shown correspond to those marked in bold in Table S3. Panel c shows the mean changes in lifespan induced by the different dilutions (more details and statistics of the assays in Tables S1 and S3). Panel d shows the SCA-1 mRNA expression at day 5 of adult life in control worms or in worms treated with 10% or 100% *sca-1* RNAi from day 1 of adult life.

Figure 4. Effect of SERCA inhibition on the lifespan of *aak-1;aak-2* and *nuo-6* mutants. Panels show representative survival plots corresponding to parallel lifespan trials (control vs drug) performed in *aak-1;aak-2* mutants (panels a-c) or *nuo-6* mutants (panels d-f) using either 10nM thapsigargin (panels a,d), 250μM 2,5-BHQ (panels b,e) or 10% sca-1 RNAi (panels c,f). In each panel, the trace labelled "Control" was obtained with the corresponding mutant, and the other was obtained in the same mutant treated with the drug or *sca-1* RNAi from day 1 of adult life. The trials shown correspond to those marked in bold in Table S4 (more details and statistics of all the assays in Tables S1 and S4).

879

880 **Fig. 5. Effect of *sca-1* RNAi on the lifespan of *mcu-1* and *unc-68* mutants.** Panel a shows
881 representative survival plots corresponding to parallel lifespan trials performed with N2
882 worms, N2 worms treated with 10% sca-1 RNAi, *mcu-1* mutants and *mcu-1* mutants treated
883 with 10% sca-1 RNAi from day 1 of adult life. The trials shown correspond to those marked
884 in bold in table S6. Panel b shows representative survival plots corresponding to parallel
885 lifespan trials performed with *unc-68* mutants treated or not with 10% sca-1 RNAi from day
886 1 of adult life. The trials shown correspond to those marked in bold in table S7. More details
887 and statistics of all the assays in Tables S1, S6 and S7.

888

889 **Figure 6. Effect of SERCA inhibitors on ER stress.** Panels a and b show the mean
890 fluorescence obtained from SJ4005 (expressing *hsp-4*::GFP) worms after different
891 treatments. Panel a shows the effects of 3 days treatment with thapsigargin or 2,5-BHQ. Panel
892 b shows the effects of the same treatments either in the absence or in the presence of
893 tunicamycin. Controls were added the corresponding amount of DMSO. ***, $p<0.001$. Error
894 bars are s.e.m. (n=40-42 worms analyzed in each condition). Panels c and d show the effect
895 of *sca-1* RNAi on mRNA expression of HSP-3 and HSP-4 measured by RT-qPCR at day 5
896 of adult life. Bars show mean±s.e., n=3.

897

898 **Figure 7. Cartoon showing the proposed mechanism for the effect of the SERCA**
899 **inhibitors.** Ca^{2+} transfer from ER to mitochondria takes place in the MAMs, where IP_3R in
900 the ER membrane, VDAC porins in the outer mitochondrial membrane and MCU channels
901 in the inner mitochondrial membrane create a Ca^{2+} pathway between both organelles. In panel
902 A, under control conditions, Ca^{2+} transfer from ER to mitochondria increases mitochondrial
903 metabolism and ATP production. The increase in the ATP/AMP ratio inhibits AMPK,
904 activating TORC1, which has a negative impact on lifespan, in part via inhibition of DAF-
905 16. In panel B, in the presence of the SERCA inhibitors, the decrease in the ER Ca^{2+} content
906 reduces ER to mitochondria Ca^{2+} transfer. Mitochondrial metabolism is reduced and the
907 ATP/AMP ratio decreases. AMP increase leads to activation of AMPK, inhibition of TORC1
908 and increase in lifespan, in part via DAF-16 activation.

909

910

911

912

Supplementary Data

Table S1a. Treatment of *daf-2* mutant worms with SERCA inhibitors							
DRUG	Lifespan Drug (days)	N Drug	Lifespan Control (days)	N Control	% Lifespan increase	p value Drug vs Control	**Mean % lifespan increase**
Thaps 10nM	27.5	98/110	25.3	87/99	8.6	<0,05	**13.0±2.5**
	33.2	86/107	29.4	67/91	13.1	<0,0001	
	30.2	**108/145**	**25.7**	**75/146**	**17.3**	**<0,0001**	
2,5-BHQ 250µM	28.0	83/108	25.3	87/99	10.7	<0,001	**11.4±1.3**
	32.2	77/103	29.4	67/91	9.6	<0,0001	
	29.3	**100/143**	**25.7**	**75/146**	**14.0**	**<0,0001**	

Table S1b. Treatment of *daf-16* mutant worms with SERCA inhibitors							
DRUG	Lifespan Drug (days)	N Drug	Lifespan Control (days)	N Control	% Lifespan increase	p value Drug vs Control	**Mean % lifespan increase**
Thaps 10nM	**13.0**	**87/104**	**12.2**	**81/101**	**7.0**	**<0,014**	**7.1±2.0**
	13.4	96/111	12.9	90/103	3.8	0,118	
	16.6	97/118	15.0	88/99	10.7	<0,0001	
2,5-BHQ 250µM	11.8	76/82	12.2	81/101	-2.9	0,128	**5.1±4.7**
	13.5	**98/114**	**12.9**	**90/103**	**4.7**	**<0,04**	
	17.0	80/95	15.0	88/99	13.4	<0,0001	

Table S1c. Treatment of *sir-2.1* mutant worms with SERCA inhibitors							
DRUG	Lifespan Drug (days)	N Drug	Lifespan Control (days)	N Control	% Lifespan increase	p value Drug vs Control	**Mean % lifespan increase**
Thaps 10nM	19.8	97/107	17.9	88/101	10.4	<0.01	**9.4±0.9**
	23.4	90/104	21.7	81/90	7.5	0.05	
	17.6	**97/108**	**16.0**	**83/86**	**10.1**	**<0.001**	
2,5-BHQ 250µM	18.0	100/103	17.9	88/101	0.2	0.9	**10.2±5.9**
	23.9	98/107	21.7	81/90	9.8	<0.02	
	19.3	**90/98**	**16.0**	**83/86**	**20.6**	**<0.0001**	

Table S1. Lifespan assays performed with SERCA inhibitors in daf-2 and daf-16 mutant worms. The table shows the drug concentration used in each series of assays, the half-life (T½) of the worms incubated with the drug obtained from the Kaplan-Meier analysis, the number of worms in the drug-containing assay (final/total), the half-life (T½) of the control worms, the number of worms in the control assay (final/total), the %

increase in the half-life, the statistical significance of the difference between control and treated worms, obtained from the log-rank test, and the mean±s.e. increase in half-life from all the series made with the same drug concentration. In bold, series shown in the survival plots of Fig. 1.

Table S2a. Treatment of *daf-15/unc-24* mutant worms with SERCA inhibitors

DRUG	Lifespan Drug (days)	N Drug	Lifespan Control (days)	N Control	% Lifespan increase	p value Drug vs Control	**Mean % lifespan increase**
Thaps 10nM	**19.9**	**71/90**	**19.6**	**69/91**	**1.3**	**0,8**	**-4.8±6.1**
	18.0	89/104	20.2	82/93	-10.9	<0,0001	
2,5-BHQ 250µM	17.7	85/103	18.2	81/100	-2.8	0.38	**-1.7±1.2**
	19.8	**77/100**	**19.6**	**69/91**	**0.7**	**0.82**	
	19.6	79/96	20.2	82/93	-3.0	0.17	

Table S2b. Treatment of *rsks-1* mutant worms with SERCA inhibitors

DRUG	Lifespan Drug (days)	N Drug	Lifespan Control (days)	N Control	% Lifespan increase	p value Drug vs Control	**Mean % lifespan increase**
Thaps 10nM	**24.7**	**117/153**	**22.2**	**116/143**	**11.3**	**<0.001**	**10.1±2.1**
	23.6	144/151	22.3	146/155	6.1	<0.01	
	19.9	139/155	17.6	132/154	13.0	<0.0001	
2,5-BHQ 250µM	24.8	142/155	19.8	135/146	24.8	<0.0001	**24.9±2.2**
	30.1	134/155	24.2	116/146	24.7	<0.0001	
	28.9	152/159	22.2	116/143	30.5	<0.0001	
	26.7	**133/141**	**22.3**	**146/155**	**19.7**	**<0.0001**	

Table S2. Lifespan assays performed with SERCA inhibitors in daf-15/unc-24, rsks-1 mutant worms. Details as in Table S1. In bold, series shown in the survival plots of Fig. 2.

Table S3. Treatment of N2 worms with *sca-1* RNAi							
sca-1 dilution	Lifespan sca-1 (days)	N Drug	Lifespan Control (days)	N Control	% Lifespan increase	p value sca-1 vs Control	**Mean % lifespan change**
5%	17.6	65/82	14.5	72/82	21,3	<0,001	**19.2±2.1**
	17.7	86/89	14.4	97/107	23,4	<0,001	
	18.3	**73/80**	**15.5**	**71/74**	**18,4**	**<0,001**	
	17.9	66/82	15.7	75/84	13.9	<0,001	
10%	17.8	76/83	14,5	72/82	23,2	<0,001	**19.3±2.6**
	18.0	77/84	14.4	97/107	25.3	<0.001	
	18.2	**75/76**	**15.5**	**71/74**	**17.5**	**<0.001**	
	17.5	78/85	15.7	75/84	11.7	<0.001	
	18.7	76/79	14.9	84/87	25.5	<0.001	
	19.7	158/186	17.5	161/165	12.6	<0.005	
25%	19.9	48/50	21.7	21/29	-8.3	<0.005	**-13.7±2.4**
	17.8	71/81	23.0	41/61	-22.5	<0.001	
	18.8	136/160	22.0	127/160	-14.9	<0.001	
	19.9	62/69	22.2	63/71	-10.7	<0.001	
	18.2	62/87	20.7	62/73	-12.3	<0.001	
50%	**18.0**	**60/66**	**20.8**	**38/49**	**-13.7**	**<0.001**	**-22.7±3.8**
	17.5	79/87	21.7	21/29	-19.2	<0.001	
	16.0	64/67	23.0	41/61	-30.1	<0.001	
	14.4	72/90	19.9	42/65	-27.7	<0.001	
75%	**17.7**	**30/37**	**20.8**	**38/49**	**-15.1**	**<0.001**	**-18.1±3.1**
	18.5	64/69	21.7	21/29	-14.8	<0.001	
	17.4	79/82	23.0	41/61	-24.4	<0.001	
100%	**19.0**	**46/52**	**20.8**	**38/49**	**-8.9**	**<0.005**	**-18.0±3.7**
	18.4	82/88	21.7	21/29	-15.1	<0.001	
	17.4	59/65	23.0	41/61	-24.1	<0.001	
	15.2	72/84	19.9	42/65	-23.7	<0.001	

Table S3. Lifespan assays performed with several dilutions of *sca-1* RNAi in wild-type N2 worms. Details as in Table S1. In bold, series shown in the survival plots of Fig. 3.

Table S4a. Treatment of *aak-1;aak-2* double mutant worms with SERCA inhibitors							
DRUG	Lifespan Drug (days)	N Drug	Lifespan Control (days)	N Control	% Lifespan increase	p value Drug vs Control	**Mean % lifespan increase**
Thaps 10nM	14.8	89/112	15.0	102/121	-1.2	0.4	**0.3±1.5**
	13.8	**86/117**	**13.6**	**86/109**	**1.7**	**0.6**	
2,5-BHQ 250µM	15.3	99/154	15.6	93/156	-1.7	0.2	**-1.0±1.0**
	14.5	**105/122**	**14.5**	**101/112**	**0.5**	**1.0**	
	14.5	102/118	15.0	102/121	-3.5	<0.02	
	13.7	98/115	13.6	86/109	0.9	0.7	
sca-1 RNAi 10%	12,3	107/120	12,6	147/156	-2,5	<0.05	**-1.6±0.5**
	13,1	137/173	13,3	144/177	-1,7	0.32	
	12,6	**84/128**	**12,6**	**129/159**	**-0,7**	**0.54**	

Table S4b. Treatment of *nuo-6* mutant worms with SERCA inhibitors							
DRUG	Lifespan Drug (days)	N Drug	Lifespan Control (days)	N Control	% Lifespan increase	p value Drug vs Control	**Mean % lifespan increase**
Thaps 10nM	**25.7**	**94/105**	**26.4**	**76/102**	**-2.7**	**0.14**	**-2.6±3.7**
	26.0	89/101	25.1	70/89	3.7	0.9	
	21.7	90/100	23.8	80/104	-9.0	<0.001	
2,5-BHQ 250µM	24.5	90/103	26.4	76/102	-7.1	< 0.01	**-4.4±2.1**
	25.1	83/92	25.1	70/89	-0.2	0.1	
	22.4	**75/93**	**23.8**	**80/104**	**-5.8**	**0.07**	
sca-1 RNAi 10%	24.1	116/125	30.3	120/124	-20.6	<0.001	**-11.9±4,4**
	23.8	74/93	25.6	59/75	-7,2	0.1	
	25.4	**106/127**	**27.6**	**128/144**	**-8.0**	**<0.005**	

Table S4. Lifespan assays performed with SERCA inhibitors and sca-1 RNAi in *aak1;aak2* double mutant worms and *nuo-6* mutant worms. Details as in Table S1. In bold, series shown in the survival plots of Fig. 4.

Table S5. Control experiment: effect of treatment with SERCA inhibitors in wild-type worms fed with dead OP50							
DRUG	Lifespan Drug (days)	N Drug	Lifespan Control (days)	N Control	% Lifespan increase	p value Drug vs Control	Mean % lifespan increase
Thaps 10nM	23.3	75/105	22.4	81/107	4.3	0.06	7.5±3.2
	23.6	**73/89**	**21.3**	**84/100**	**10.8**	**<0.002**	
2,5-BHQ 250µM	26.0	79/102	22.4	81/107	16.2	<0.0001	18.8±2.5
	25.8	**74/100**	**21.3**	**84/100**	**21.3**	**<0.0001**	

Table S5. Lifespan assays performed with SERCA inhibitors in wild-type worms fed with dead OP50. Details as in Table S1. In bold, series shown in the survival plots of Fig. S1.

Table S6. Effect of *sca-1* RNAi on *mcu-1* mutants									
	Lifespan Treatm. (days)	N Treat	Lifespan Control (days)	N Contr	% Lifespan increase	p value vs N2	p value vs *sca-1*	p value vs *mcu-1*	**Mean % lifespan increase**
sca-1	18.7	76/79	14.9	84/87	25.5	<0.001		ns	
mcu-1	16.9	97/99	14.9	84/87	13.1	<0.001	ns		
sca-1+ *mcu-1*	20.0	80/85	14.9	84/87	34.2	<0.001	<0.05	<0.001	
sca-1	19.7	158/ 186	17.5	161/ 165	12.6	<0.005		ns	**sca-1 15.2±5.3**
mcu-1	19.0	165/ 188	17.5	161/ 165	8.5	<0.001	ns		**mcu-1 10.9±1.3**
sca-1+ *mcu-1*	20.8	152/ 162	17.5	161/ 165	18.5	<0.001	<0.001	<0.05	**sca-1 +mcu-1 23.3±5.5**
sca-1	**20.0**	**146/ 162**	**18.6**	**126/ 156**	**7.6**	**<0.05**		**<0.05**	**mean±s.e**
mcu-1	**20.7**	**143/ 151**	**18.6**	**126/ 156**	**11.0**	**<0.001**	**<0.05**		
sca-1*+ *mcu-1	**21.8**	**113/ 120**	**18.6**	**126/ 156**	**17.1**	**<0.001**	**<0.001**	**<0.05**	

Table S6. Lifespan assays performed with *mcu-1* mutants with or without 10% *sca-1* RNAi. N2 wild-type worms were carried out in parallel as a control. Details as in Table S1. In bold, series shown in the survival plots of Fig. 5.

Table S7. Treatment of *unc-68* mutants with *sca-1* RNAi							
sca-1 dilution	Lifespan *unc-68*+ *sca-1* RNAi (days)	N Treat	Lifespan *unc-68* (days)	N Control	% Lifespan increase	p value *sca-1* vs Control	**Mean % lifespan change**
10%	15.7	129/141	14.5	140/154	8.7	<0,001	**8.0±0.4**
	17.7	**113/129**	**16.5**	**130/147**	**7.8**	**<0.001**	
	18.7	140/148	17.4	138/145	7.4	<0.001	

Table S7. Lifespan assays performed with *unc-68* mutants with or without 10% *sca-1* RNAi. Details as in Table S1. In bold, series shown in the survival plots of Fig. 5.

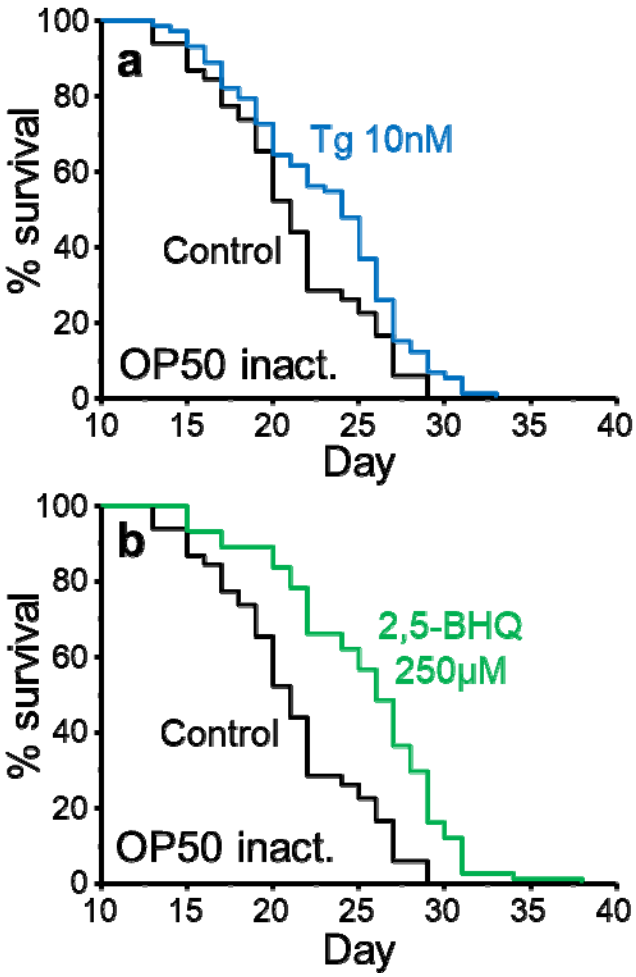

Figure S1. Effect of SERCA inhibitors on the lifespan of wild-type *C. elegans* worms grown with inactivated OP50. Panels show representative survival plots corresponding to parallel lifespan trials (control vs drug) performed in *C. elegans* worms grown with inactivated OP50 using either 10nM thapsigargin (panel a), 250µM 2,5-BHQ (panel b) or 250µM 2,6-BHQ (panel c). The trials shown correspond to those marked in bold in Table S5 (more details of all the assays in Table S1).

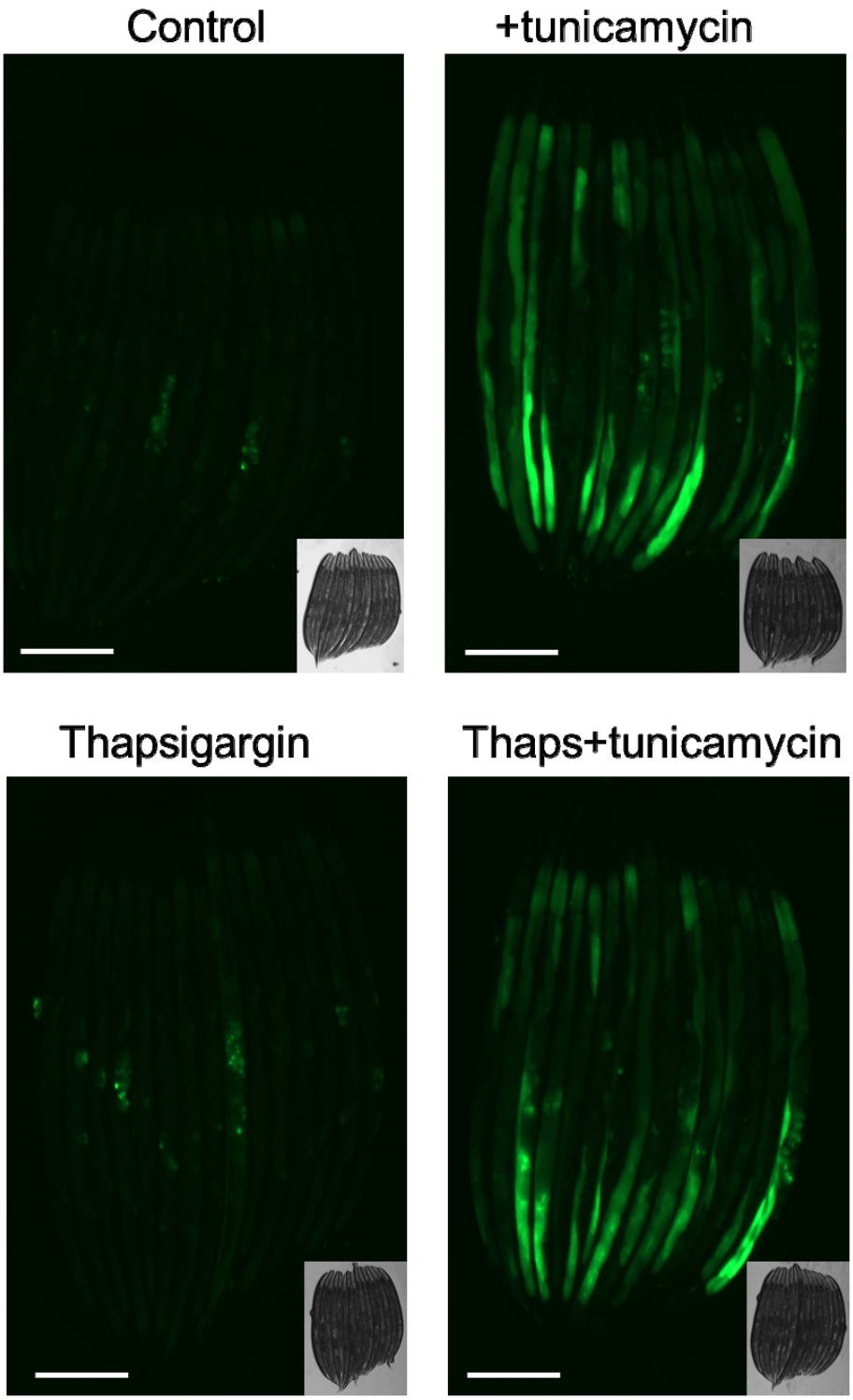

Fig. S2a. Effect of thapsigargin on ER stress. SJ4005 worms were treated with or without thapsigargin and some of the worms in each condition were also treated with tunicamycin, as detailed in Methods. The level of fluorescence indicates the expression of *hsp-4*::GFP as an ER stress reporter. The insets show the brightfield image. Bar is 200µm.

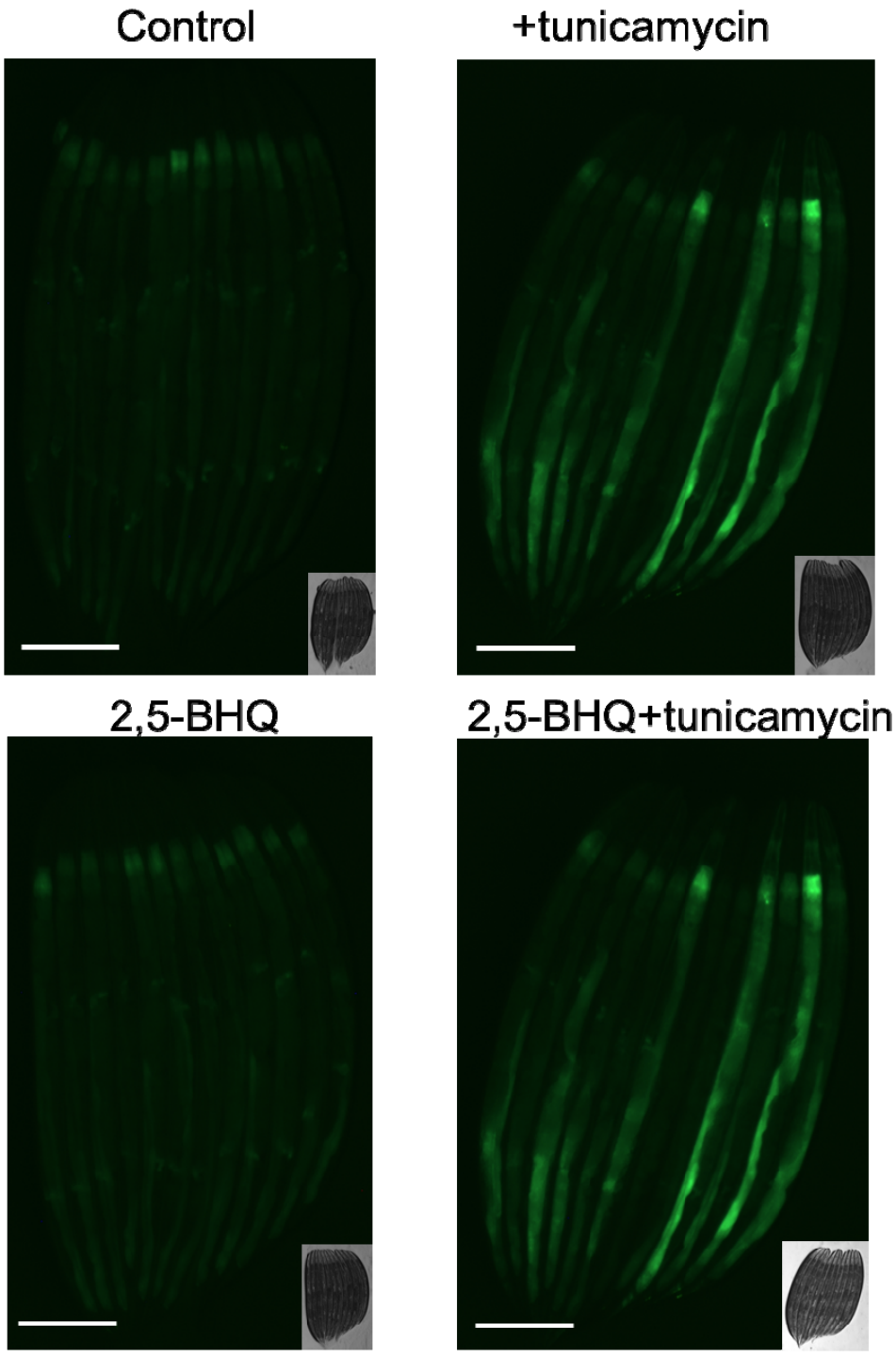

Fig. S2b. Effect of 2,5-BHQ and 2,6-BHQ on ER stress. SJ4005 worms were treated with or without the compounds and some of the worms in each condition were also treated with tunicamycin, as detailed in Methods. The insets show the brightfield image. Bar is 200μm.